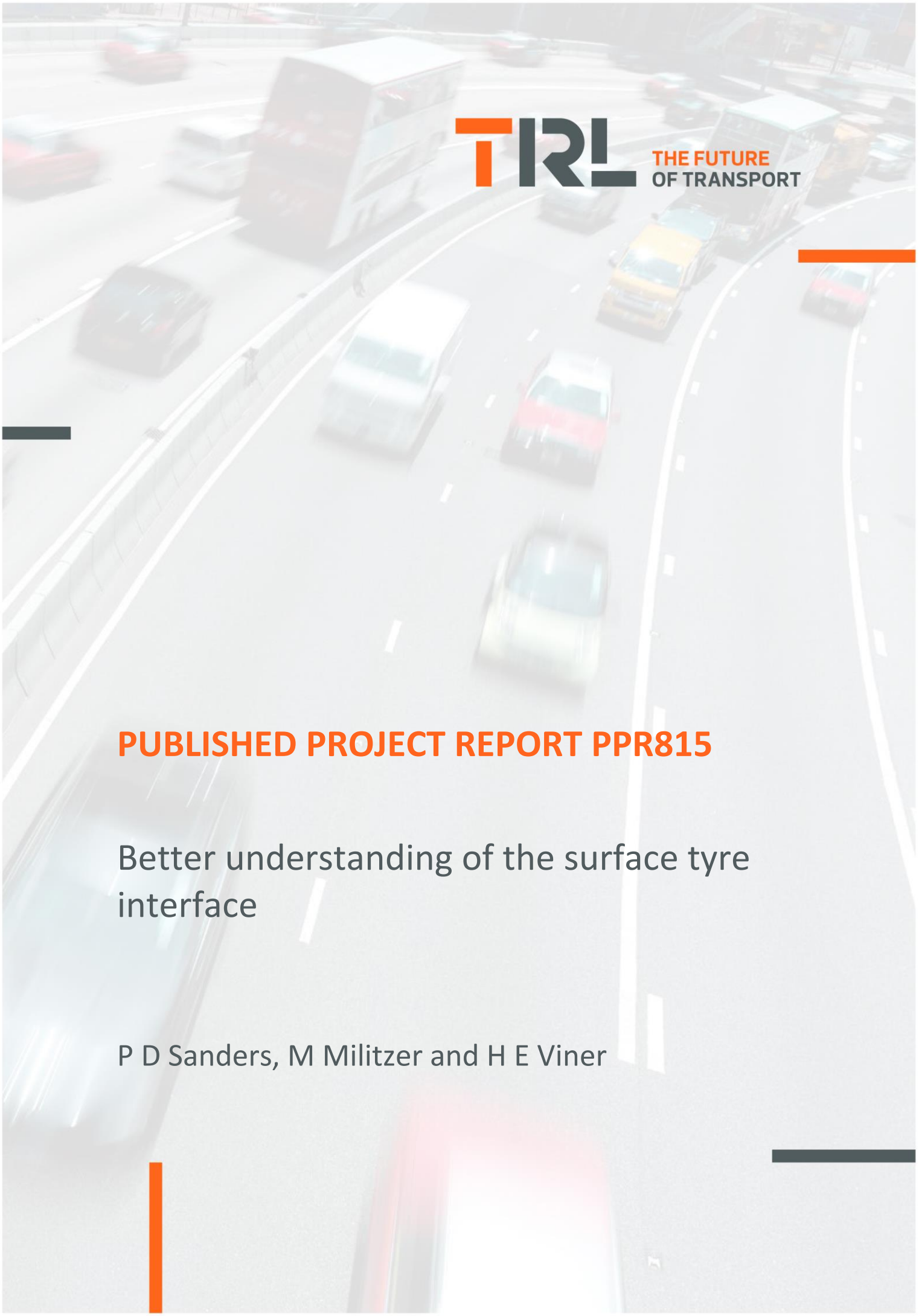

THE FUTURE OF TRANSPORT

PUBLISHED PROJECT REPORT PPR815

Better understanding of the surface tyre interface

P D Sanders, M Militzer and H E Viner

Report details

Report prepared for:	Highways England, Safety, Engineering and Standards		
Project/customer reference:	626(4/45/12)		
Copyright:	© Transport Research Laboratory		
Report date:	February 2017		
Report status/version:	Published		
Quality approval:			
(Project Manager)	Stuart McRobbie	(Technical Reviewer)	Martin Greene

Disclaimer

Contents amendment record

This report has been amended and issued as follows:

Version	Date	Description	Editor	Technical Reviewer
1.0	10/10/2016	Working draft	PS/MM	HV
1.1	19/12/2016	Working draft	HV	N/A
1.2	23/12/2016	Working draft	PS	
2.1	05/01/2017	Complete draft for client review	PS/HV	HV
2.2	26/01/2017	Client review	OA	
3.0	09/02/2017	Edits following client review	PS	MG

Document last saved on:	28/04/2017 16:58
Document last saved by:	McRobbie, Stuart G

Table of Contents

Executive summary

The friction developed between the road surface and vehicles' tyres provides motorists with the reaction forces necessary for manoeuvring. On the English Strategic Road Network (SRN) this is managed through the specification of low speed skid resistance, texture depth and the polishing resistance properties of aggregates.

A combination of changes to the SRN (motorway layout and pavement surface type) and the vehicle fleet (anti-lock braking systems and electronic stability control systems) in recent years makes it appropriate to review the current approach. The work reported here was commissioned by Highways England to investigate how surface characteristics affect the ability of road users to control their vehicles. This was achieved through the completion of the following tasks:

- A literature review was conducted to identify studies assessing the relationship between pavement performance and vehicle demand.
- A methodology was created to define and assess the relationships between friction, wheel slip and vehicle speed using historical friction measurements. This facilitated a more detailed understanding of the characteristics of different surfacing materials than can be obtained from the standardised measurement of skid resistance and texture depth.
- The relationships between friction, wheel slip and vehicle speed were used to identify typical material behaviours and the relationship with texture and low speed skid resistance.
- All the information from the above tasks was combined to determine how significant the low speed skid resistance and texture depth are for road users carrying out braking manoeuvres from different initial speeds.
- A robust approach was developed for estimating the implications of delivering different levels of friction and texture, including a reduction from current requirements.

From the work carried out the following conclusions were made:

- Concrete and asphalt materials exhibit markedly different friction performance. Further work should be undertaken to assess the effect of material design on the friction performance of TSCS materials, which varies considerably.
- The friction prediction model developed performs well overall in predicting friction over a wide range of slip ratio and vehicle speed, from inputs of low speed skid resistance and texture depth. However, it is less accurate at low slip (below 5%) and low, low speed friction (around 0.30 units SC(50)).
- Whilst low speed skid resistance and texture depth both contribute to the braking performance, the importance of texture depth seems particularly significant and texture depth is better able to compensate for lower levels of low speed skid resistance than vice versa.

- There appears to be an optimum contribution of low speed skid resistance and texture depth to braking distance, taking account of the vehicle speed and the performance of different surfacing materials.
- The use of driver aids designed to exploit peak friction has a substantial benefit on the braking performance of vehicles. A wide uptake (approaching 100%) of driver aids could allow for a reduction in the friction requirements on the SRN. However, information on the current and projected distribution of vehicles with driver aids would be needed before making changes to specifications.

1 Introduction

The friction developed between the road surface and vehicles' tyres provides motorists with the reaction forces necessary for manoeuvring. Maintaining appropriate and predictable friction conditions is an important contributor to road user safety. On the English Strategic Road Network (SRN) this is managed through the specification of low speed skid resistance (HD28 Skidding resistance, 2015), texture depth, (HD29 Data for pavement assessment, 2008) and (Manual of Contract documents for Highway Works, 2008), and the polishing resistance properties of aggregates (HD36 Surfacing materials for new and maintenance construction, 2006). The requirements have been in place and have remained relatively unchanged for some time.

A combination of changes to the SRN (motorway layout and pavement surface type) and the vehicle fleet (anti-lock braking systems and electronic stability control systems) in recent years makes it appropriate to review the current approach. It is possible that, with the developments to roads and vehicles, the specification of skid resistance and texture measurements may be excessively cautious, or that these characterisations may not be the most appropriate for mitigating risk. Since the texture depth requirement, in particular, is associated with a trade off as regards to the properties of noise, rolling resistance and durability, there could be substantial potential benefits as a result of amending the specifications.

This work was commissioned by Highways England to update the current knowledge of how surface characteristics affect the ability of road users to control their vehicles through the manoeuvres necessary for them to complete their journey (acceleration / braking / cornering). The work comprises a literature review, reported in chapter 4 and an investigation into the friction characteristics of common surfacing materials, and how they could influence vehicle braking characteristics. This is the major part of the study and is reported in chapters 5 to 8. A parallel investigation of the relationship between collision risk and skid resistance is reported separately (Wallbank *et al.*, 2016).

2 Background

The instantaneous friction available for vehicle manoeuvring depends on a complex mix of tyre, vehicle and surface characteristics. Measurements of the road surface contribution to friction are therefore carried out under standardised conditions to eliminate, as far as possible, the variation from other sources. These measurements are denoted "skid resistance" and, in network analyses, relate to average crash rates (Wallbank *et al.*, 2016). However, they do not accurately represent the friction available to road users in a particular situation. This work has been carried out to better understand the relationship between the skid resistance measurements made for asset management purposes, and the friction available to road users for specific manoeuvres.

Skid resistance is typically measured in one of the following ways:

- In side-force tests, a test tyre is angled with respect to the direction of travel, thereby creating a slip between the tyre and road surface, for example SCRIM (BSI, 2006), for which the standard test speed is 50 km/h.
- In fixed-slip tests, a test wheel rotates in the direction of travel and is forced to slip over the road surface at a constant fraction of the vehicle velocity, for example the GripTester (BSI, 2000). Measurements are typically made at 50km/h.
- In locked-wheel tests, such as those made with the Pavement Friction Tester (PFT), measurements are made over a full locked wheel braking cycle. During testing, the tyre/road contact patch is forced through a full braking cycle from instantaneously stationary (free rolling) to moving at the speed of the tow vehicle (fully locked) (ASTM, 2011). High speed friction measurements are typically made at 90km/h.

These skid measurement devices only characterise a limited combination of the vehicle speeds and wheel slips that are available to road users. It is plausible therefore that, depending on the manoeuvre they are attempting to execute, road users may sample combinations of vehicle speed and wheel slip that are not characterised by the standard skid resistance test methodologies.

The work presented in this report will focus heavily on data collected using the Highways England PFT device, Figure 2-1. Measurements made with this device are performed in accordance with the procedure set out in ASTM E-274 (ASTM, 2011) and utilise a smooth treadless tyre as per ASTM E-524 (ASTM, 2008). For each test cycle the test wheel held on the trailer is braked, causing it to lock and skid for approximately two seconds. During a test cycle the vertical and horizontal load forces placed upon the test wheel are recorded, alongside vehicle and wheel speed every 0.01 seconds. Standard tests are conducted in wet conditions by pumping water (from a tank in the tow vehicle), at a controlled rate producing a nominal water film thickness of 1.0mm.

Measurements made with this device can be conducted at any practicable speed, therefore by conducting multiple measurements on the same surface it is possible to capture information at a range of test speeds. It is this methodology which forms the basis of the bulk of the work reported herein.

Figure 2-1 The Pavement friction tester

3 Research aims

The key aims of this work are to:

- Conduct a literature review to identify works assessing the relationship between pavement performance and vehicle demand.
- Define and assess the relationships between friction, wheel slip and vehicle speed.
- Use the relationships between friction, wheel slip and vehicle speed to identify typical material behaviours and the relationship with texture and low speed skid resistance.
- Combine the information from the above tasks to determine how significant the skid resistance and texture depth are for road users carrying out different manoeuvres.
- Develop a robust approach to estimating the implications of delivering different levels of friction and texture, including a reduction from current requirements. Provide recommendations to Highways England on changes to current standards and methods for implementation.

4 Literature review

This chapter presents the results of a literature review carried out to inform the understanding of how surface characteristics influence vehicle handling in different manoeuvres. The study started by defining tyre/road friction and exploring its contributory factors. Friction and tyre models used in industry were then explored to gain an insight into the parameters used and how these relate to friction prediction systems. The study concludes with a discussion of driver aids and how these affect tyre/road friction.

4.1 General principles of tyre/road friction

Tyre/road friction is a result of the interaction between the tyre and the road surface, the resistive force (friction) being generated by the movement of the tyre across the road surface. The frictional force is generated at the interface of the tyre and the road, in a direction opposing the direction of travel, and is the interaction which enables vehicle manoeuvres and also determines the stopping distance (Hall *et al.*, 2009).

Friction can be characterised by the non-dimensional coefficient μ, which is determined by the proportion of the horizontal friction force H to the vertical load V as shown in Figure 4-1.

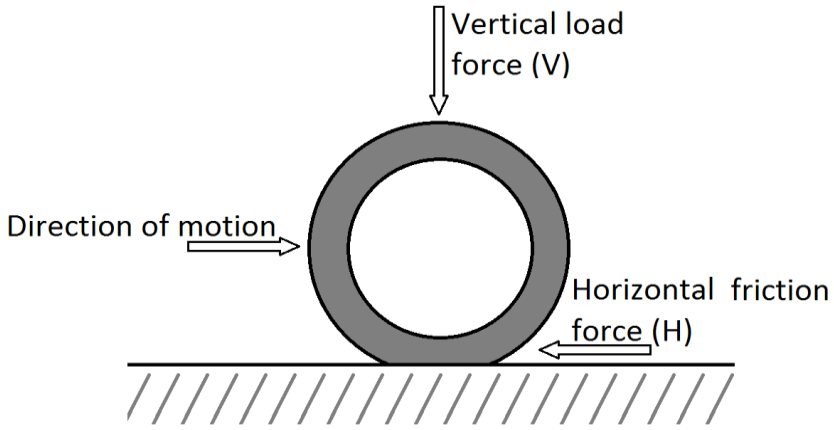

Figure 4-1 Force diagram for a roatating wheel

The speed of the tyre in relation to the pavement surface speed is referred to as slip speed, as described in Equation 4-1. It is also commonly expressed as a ratio or percentage of the vehicle speed.

$$S = V - Vp = V - (0.68 \times \omega \times r)$$

Where:

- S = Slip speed (miles/hour)
- V = Vehicle speed (miles/hour)
- V_p = Average peripheral speed of the tyre (miles/hour)
- ω= Angular velocity of the tyre [rad/sec]
- r = Average radius of the tyre (ft)

Equation 4-1 Calculation of wheel slip (Hall *et al.*, 2009)

The coefficient of friction between a tyre and the pavement changes with varying slip. It increases rapidly with increasing slip to a peak value, known as peak friction, that usually occurs between 10 and 20 percent slip. The friction then decreases to a value known as the coefficient of sliding friction or locked-wheel friction, which occurs at 100 percent slip.

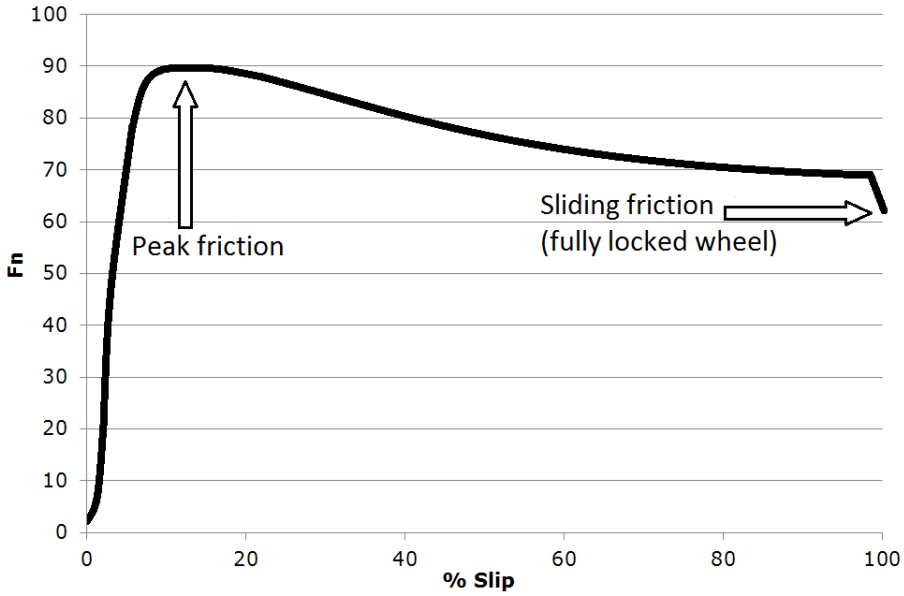

Figure 4-2 Idealised friction versus tyre slip reationship

Peak and sliding friction vary little on dry surfaces and are relatively unaffected by variation in speed. Effects are more marked on wet roads, with locked-wheel friction being lower than peak friction, and both generally decreasing with an increase in speed. These differences depend on vehicle speed and tyre properties, but also on the road surface properties. According to Henry (2000) and Flintsch et al. (2012) measurements made on the left side of the peak (lower slip ratios) are mainly influenced by tyre properties, whereas measurements on the right hand side (higher slip ratios) mainly depend on the macrotexture of the road surface.

4.2 Factors influencing tyre/road friction

As the friction coefficient is defined by the interaction between the road surface and the tyre, the friction depends on various factors which can be grouped into four categories:

- Pavement surface characteristics
- Vehicle operational parameters
- Tyre properties
- Environmental factors

4.2.1 Pavement surface characteristics

The tyre/road friction in wet pavement conditions is greatly influenced by the texture of the road surface. The fine-scale texture on the surface of the coarse aggregate (microtexture)

interacts directly with the tyre rubber to provide adhesion. According to Hall et al. (2009) this component is especially important at low speeds but needs to be present at any speed. In general, in wet conditions, surfaces with greater macrotexture tend to provide better friction at high speeds for the same low-speed friction (Roe and Sinhal, 1998).

Sanders et al. (2014) concluded that, for most surfaces with texture depth below approximately 0.8 mm Sensor Measured Texture Depth (SMTD), friction at high speed increases linearly with texture, and for textures above 0.8 mm SMTD, friction changes little with increasing texture. However this is not always the case: (Roe and Dunford , 2012) found for certain asphalt materials with relatively low texture depth, locked-wheel friction decreases with speed but not to the extent expected from other surfaces with comparably low macrotexture.

This replicates the earlier findings of TRL367 (Roe *et al.*, 1998) which concluded that as friction falls with speed, there is also a relation between friction and texture: friction on low-textured surfaces falls more rapidly than high-textured surfaces. The effect of texture depth on loss of friction was greatest below about 0.7mm SMTD. Above this level, increased texture has a relatively small effect. This work did not assess small-sized aggregate thin surfacings but found that porous asphalt surfacings were providing higher friction levels than expected. It was also found that the texture depth has an impact on friction at low speeds.

4.2.2 Vehicle operating parameters

Vehicle parameters affecting the friction between the tyre and the road are discussed in more detail in section 4.4 and section 4.5.

4.2.3 Tyre properties

Tyre properties such as compound, pattern, tread depth, condition and pressure have an impact on the tyre/road friction. The design of the tyre tread and the condition of the tyre affect the ability of the tyre to remove water from the tyre/road interface. Especially for greater water film thicknesses, the tread depth is important at high speeds when the amount of water accumulating in front of the tyre can be greater than the water that is being removed.

Henry (1983) conducted a study comparing the locked-wheel friction performance of different tyre types. The results of the study demonstrated that locked-wheel friction at 40 miles/hour (64 km/h), measured using a smooth tyre is between 45 and 70 percent of the value measured using a new treaded tyre.

Tyre inflation pressure affects the size and distribution of the tyre/road contact patch. Under-inflation causes an increase in contact area and therefore constricting drainage channels and reducing the average contact pressure on the road surface. As a result, water can become trapped underneath the tyre and the speed at which hydroplaning is likely to occur decreases. Over-inflation however, reduces the trapping effect, reduces the contact area and increases the contact pressure, resulting in a higher hydroplaning speed (Hall *et al.*, 2009). Below hydroplaning speed, Tyrosafe report D10 (Kane et al, 2009) suggests that changes in inflation pressure over relatively wide ranges did not produce significant variations in friction on wet roads, although it did have an effect in dry conditions.

Classically, it has been suggested that two mechanisms, adhesion and hysteresis, are responsible for the generation of friction between rubber and other surfaces, and that the overall friction between tyre and road surface is the sum of these two components (Kummer, 1966). Adhesion is generated at the interface of the rubber and a dry road surface. The polymer chains within the rubber and the surface material interact on a molecular scale, causing distortion of the polymer chains and hence generating friction. This process may even involve the formation and breaking of chemical bonds. Hysteresis arises because energy is lost during the physical deformation of the bulk material by surface asperities. In this process, some of the energy that is used to deform the tyre tread when it slides over the texture is absorbed by the tyre when it returns to its original shape.

4.2.4 Environmental factors

Environmental factors such as temperature and the presence of water, or other contaminants, on the road surface also have an impact on the friction available. As tyres and asphalt road surfacings are made of visco-elastic materials, their properties are affected by temperature.

Water acts as a natural lubricant, which reduces the friction by an amount proportional to the water film thickness. On wet roads, the free rolling tyre/road interface has been characterised in terms of three regions (Moore, 1975). In the sinkage, or "squeeze-film" zone at the forward edge of the tyre/road contact area, the tyre does not make contact with the road, but floats on a thin wedge of water. The depth of water reduces progressively towards the rear of this area, as the water film is squeezed out of the interface by the tyre. In the "draping zone", the tyre makes partial contact with the asperities of the road surface, the water film having been mainly removed by the squeezing action. Finally, at the rear of the contact area, there is an area of actual contact, where most of the friction is generated.

The friction generated depends on the relative areas of these three regions, which is determined by the depth of water, the vehicle speed and the rate at which water can be dispersed from the contact area. As the vehicle speed and the amount of water increase, the contact area becomes progressively reduced until it disappears, at which point the vehicle is said to be hydroplaning.

Further environmental impacts such as the presence of snow and ice also affect the available friction by obscuring the road surface from the tyre and instead presenting the tyre with a low friction contaminant (Hall *et al.*, 2009). The presence of snow and ice is a special case and not directly related to this study.

4.3 Friction models

4.3.1 Road friction models

Several models exist for predicting pavement friction as a function of the vehicle speed and road characteristics. The most commonly reported are:

- The Rado model
- The Penn State model
- The PIARC model

The Rado model

The Rado model, also known as the logarithmic friction model, aims to model the friction path as the tyre proceeds from the free rolling to the locked-wheel condition at a single vehicle speed, Equation 4-2.

$$\mu = \mu_{peak} \times e\left[-\frac{ln\left(\frac{V_s}{S_{peak}}\right)^2}{C^2}\right]$$

Where:

- μ_{peak} = peak friction level
- V_s = the slip speed
- S_{peak} = slip speed at the peak (typically 15% of vehicle speed)
- C = Shape factor – mainly dependent on surface texture

Equation 4-2 The Rado model

The model describes two phases during the braking process. In the first phase, the tyre rotation reduces from free rolling to the peak friction state. Subsequently, the tyre slip speed reduces to the locked-wheel state (100% slip). The corresponding friction coefficient therefore increases to the peak friction level, and then decreases by the increase of the slip ratio (Wang *et al.*, 2010).

The Penn State Model

The Penn State model describes the relationship between friction and slip speed as an exponential function.

$$\mu = \mu_0 \times e\left[\frac{PNG}{100} \times S\right]$$

Where:

- μ_0 = static friction at zero speed
- S = wheel slip speed
- PNG = Percent Normalised Gradient (Equation 4-4)

Equation 4-3 The Penn State model

$$PNG = -\frac{100}{\mu}\frac{\partial \mu}{\partial S}$$

Equation 4-4 Definition of PNG

PNG was discovered to be constant with speed and correlates highly with macrotexture, therefore μ_0 could be predicted by macrotexture. Later versions of this model replaced the PNG/100 by the speed constant S_p (Henry, 2000).

The static friction coefficient μ_0 is related to pavement surface microtexture; and the speed constant is highly correlated with pavement surface macrotexture (Wang *et al.*, 2010).

The PIARC Model

The PIARC model is an adaption of the Penn State model in which the μ_0 term has been replaced to represent the friction at 60 km/h resulting in the following.

$$F(S) = F_{60}\, e^{\frac{60-S}{Sp}}$$

Where:

- F(S) = friction at slip speed S
- F_{60} = friction at 60 km/h
- S_P = IFI Speed Number, see Equation 4-6

Equation 4-5 The PIARC model

$$S_P = a + b \times Txt$$

Where:

- a and b are constants defined in ASTM standards E1845 and E965 (ASTM, 2015)
- Txt = macrotexture measurement (mm)

Equation 4-6 Definition of S_p

The PIARC experiment was conducted in 1992 and aimed to compare and harmonise texture and skid resistance measurements. The experiment resulted in the development of the International Friction Index (IFI), the aim of which was to allow skid resistance to be measured by any methodology and compared on a common scale. Tyrosafe D05 (Vos *et al.*, 2009) reported that although this approach worked to some extent the precision of the resulting common scale was not sufficient for practical application.

The IFI standardizes the way the dependency of friction on the tyre sliding speed is reported. The Speed Number (S_P) measures how strongly friction depends on the relative sliding speed of the tyre and is related to the gradient of the friction values measured below and above 37 miles/hour (60 km/hr). The S_P is reported in the range 0.6 to 310 miles/hour (1 to 500 km/hr) (Hall *et al.*, 2009).

It was confirmed that S_P is strongly influenced by the macrotexture of the surface. Besides macrotexture being a major contributor to friction, the speed number can be used to interpret the condition of the macrotexture as it changes its value over time (Hall *et al.*, 2009).

Combining the Penn State and Rado models

Combining the Penn State and the Rado models allows an approximation of the frictional performance of a surfacing when a vehicle is conducting an emergency braking. Up to the

state where the wheel is fully locked, the friction follows the Rado Model. If the breaking continues after this point, the vehicle speed decreases (being equal to slip speed) and the friction follows the Penn State model up to the point where the vehicle speed is zero (Henry, 2000). This process is shown graphically in Figure 4-3 where an example of the friction estimated by the Penn State and Rado models has been given.

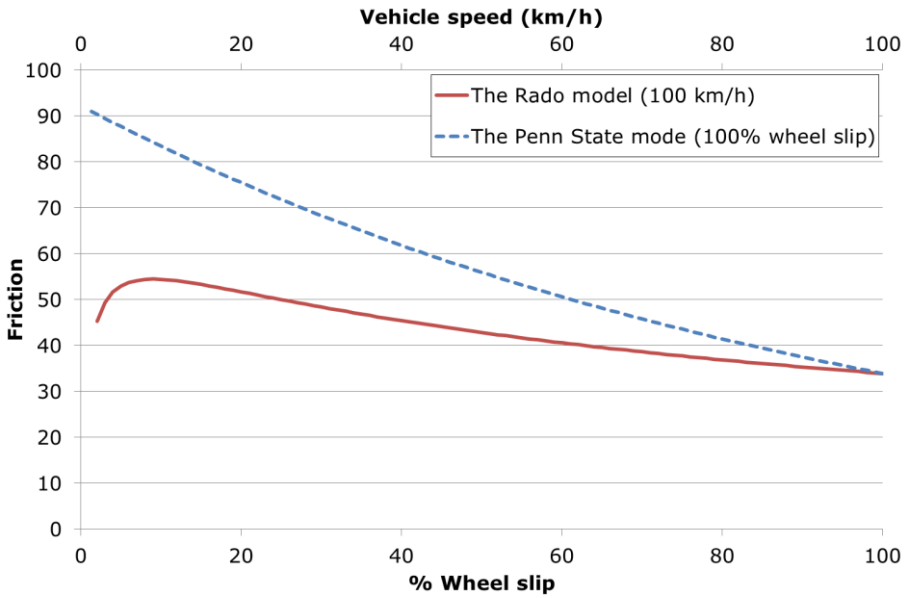

Figure 4-3 Combining the Penn State and Rado models

4.3.2 Tyre/road interaction models

Tyre models are used in vehicle dynamics to predict tyre performance in terms of traction and stability control. Overall, Wong (1993) states that tyre models should consider the composite structure of the tyre, the deformation as well as the near-incompressibility and the non-linearity of rubber material.

Many models describing tyre dynamics have been developed, ranging in complexity from basic models having a single contact point with the road surface to more complex 3-D models which take the deformation, tyre properties such as rim and reinforcements, and pneumatic pressure into consideration (Wang *et al.*, 2010).

Most tyre models are developed for tyre design purposes and aim to predict the level of deformation and the interaction between the tyre components. In 2010 a 3D tyre-pavement interaction model was developed by Wang et al. in order to analyse the forces and stresses generated between the tyre and road surface during vehicle manoeuvring (free rolling, braking/acceleration, and cornering).

Wang defined tyre-pavement interaction as a function of three nonlinear factors: material, geometry and the contact itself. For the simulation the pavement was modelled as a multi-layer structure that has nonlinear material properties for each of the layers. The structure of the tyre is composed of a complex structure including the rubber and the reinforcement. Overall, it was found that, with an increase in surface friction, the lateral contact stresses, at various manoeuvres, and the vertical contact stresses, for cornering manoeuvres, increase.

The model summarised above and all of the other tyre/road interaction models identified as part of this review modelled the road surface contribution to friction as a pre-determined value only. This approach requires the friction of the road surface to be known in advance and so goes little way to adding to the understanding of road surface properties that contribute to friction.

4.4 Active vehicle safety systems

4.4.1 Friction estimation

Friction estimation is used by active vehicle safety systems such as Anti-lock Braking Systems (ABS) or Electronic Stability Control (ESC). Friction estimation systems can be classified into three groups (Singh and Taheri, 2015):

- Vehicle Based Systems - These systems use the longitudinal and lateral motions of the vehicle and the differential speed of the vehicle wheels (wheel slip percentage) as inputs to a friction estimation algorithm.
- Wheel Based Systems - Measurement system that utilises a redundant wheel and is appropriate for heavy duty trucks.
- Tyre Based Systems - Measurement of tyre deformation.

The common feature of all friction estimation systems is that friction is not measured directly, rather inferred from other properties.

FRICTION was an EU funded project aiming to develop an on-board system for measuring and estimating tyre/road friction and therefore to enhance the performance of vehicle integrated and cooperative safety systems. The programme was based on the preceding project APOLLO, which focused on the development of a tyre sensor for the friction estimation (Koskinen and Peussa, 2004).

The FRICTION system works around three parameters: friction currently used (tyre/road forces currently used), friction available (remaining potential) and friction potential (maximum tyre/road friction available), see Figure 4-4.

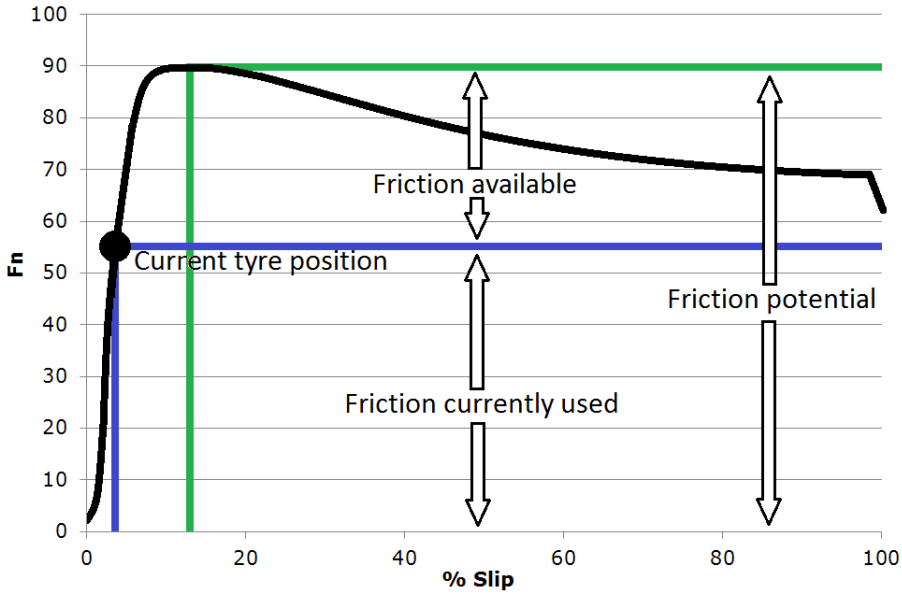

Figure 4-4 Summary of FRICTION parameters

The friction used is estimated using standard vehicle based driving dynamic sensors, such as those used for ABS or ESC systems. The friction potential is estimated using more coarse methods than those used to estimate friction used. The inputs used for the estimation of friction potential are the presence of environmental contaminants such as water or snow and the texture depth of the road surface. Measurement of these properties requires sensors not commonly available on vehicles, such as weather information systems and triangulation lasers.

4.4.2 Vehicle dynamic control

Vehicle dynamics stability control systems regulate the transmitted tyre forces which depend on the slip ratio between the tyre and the road. The primary systems in terms of driving dynamics and driving safety are (Koskinen and Peussa, 2004):

- Antilock Braking System (ABS)
- Traction Control System (TCS)
- Electronic Stability Control (ESC)
- Adaptive Cruise Control (ACC)

This section will discuss each of these systems in more detail focussing on the relationship with friction.

Antilock Braking System (ABS)

Antilock braking systems aim to diminish the loss of friction caused by sliding. It operates at the front side of the peak friction curve and causes the brakes to be applied and released in such a way that the slip is held near the peak. This ensures that the peak friction is not exceeded which would result in a loss of steering control.

The brakes are released before the peak friction is reached and are applied at a set time or percentage slip below the peak, the exact points are subject to propriety manufacturer design.

As described by (Henry, 2000), the ABS friction curve follows the Rado model, described in Equation 4-2, up to a set percentage slip whilst the vehicle speed is reducing. At this point the brake is released and the wheel slip drops, before the brake is reapplied; the cycle then repeating for a lower vehicle speed.

The control of an ABS system is, however, considered a highly nonlinear control problem as the relationship between friction and slip is complex. Furthermore the velocity of the wheel relative to the vehicle, as well as the friction, cannot be measured directly and therefore have to be estimated or inferred by sensor measurements. As a result, different control approaches have been developed (Aly *et al.*, 2011).

Traction Control System (TCS) and Electronic Stability Control (ESC)

Traction control and electronic stability control systems use the same premise of wheel slip detection and control as ABS, controlling individual wheel braking and power delivery to maintain wheel slip and therefore vehicle control. The differentiator between these systems is that ABS is activated only when the vehicle brakes are used manually, whereas TCS and ESC are always active.

The six main components of an ESC system are: wheel speed sensors, a control module, a steering angle sensor, a yaw rate sensor, an accelerometer, and the hydraulic modulator. The hydraulic modulator is the same one used in an ABS system, meaning that ESC adds only the yaw sensor, an accelerometer, and steering angle sensor to a standard ABS system. The control module recognizes the discrepancy between the intended path (communicated by the steering angle sensor) and the actual path (communicated via the yaw rate sensor) and sends a signal to the hydraulic unit, directing it to alter the braking power of individual wheels to achieve the desired response.

For example, if a driver turns the wheel very abruptly to the left, the vehicle may initially under steer. In this case, since the front tyres do not yet have enough traction and they slide, the vehicle therefore continues to move forward rather than turning left. The control module recognizes the discrepancy and directs the hydraulic unit to increase braking power to the left rear wheel. This causes the vehicle to rotate left (the desired response). If necessary, the control module will also reduce engine power by sending a signal to the throttle actuator.

Adaptive Cruise Control (ACC)

Adaptive Cruise Control (ACC) allows the vehicle to keep a constant speed until sensors detect an obstacle ahead. The speed is then adapted in a way that the distance to the obstacle remains constant. The system aims to keep the distance to the obstacle at a level allowing for safe braking in an emergency.

Braking distance can simply be calculated by the velocity and the maximum friction available indicating that, besides speed, the most influencing parameter is friction. If it is generally assumed to be a constant high value, then systems could potentially start braking too late. The calculation of the braking distance could be more precise if information about the road

friction was available (Koskinen & Peussa, 2004), enabling the systems to be used to their full potential.

General

ABS, TCS and ESC already contain friction estimation algorithms and generally their performance is difficult to improve (without better knowledge of the surface characteristics). Knowledge of a more accurate friction potential would aid the operation in their first cycles: ABS would benefit on ice by not braking too hard, and TCS could similarly limit excessive acceleration, especially when switching gears (Koskinen & Peussa, 2004).

A friction estimation system might also improve ESC algorithms by providing more accurate information about the forces and friction potential for each tyre. However, the main benefit of friction estimation system is considered to be preventing dangerous manoeuvres rather than helping to correct them (Koskinen & Peussa, 2004).

In spite of this, it appears that the friction coefficient is generally based on estimation, with no detailed analysis about the interaction between tyre, texture and friction apart from dry, wet and contaminated road surfaces. Even though tyre based algorithms exist, according to Erdogan (2009) none of these systems are mature and reliable enough to be adapted to active safety systems.

4.5 Friction demands for manoeuvring

Rolling resistance

A small amount of friction, rolling resistance, is developed between the tyre and the road surface for a tyre rolling in a straight line, as the contact area is instantaneously stationary. However, for manoeuvres involving change of speed or direction of the vehicle, the application of brakes or steering results in forces developing between the tyre and road that may enable the vehicle to carry out the manoeuvre. Longitudinal friction forces are generated when operating in the constant-brake mode, lateral or side-force friction occurs as a result of steering manoeuvres.

Straight line braking

For a braking manoeuvre the reacting force increases with the increase in braking force up to a point at which the friction available between the road surface and the tyre is exceeded, the peak friction. Flintsch, et. al. suggest that this point occurs generally between 18 and 30 percent slip. The tyre slips over the road as it continues to slow down relative to the vehicle speed. Eventually a locking of the wheel occurs at which time the tyre does not rotate anymore resulting in the skidding of the tyre/road contact patch across the road surface (Flintsch, et al., 2012).

Cornering

For a vehicle steering around a curve or carrying out a lane change manoeuvre an additional force is generated at the tyre/road interface, called lateral (side-force) friction. The relationship between vehicle speed, curvature and friction can be expressed as per Equation 4-7.

$$F_S = \frac{V^2}{15R} - e$$

Where:

- F_S = Side friction
- V = Vehicle speed (miles/hour)
- R = Radius of the path of the vehicle's centre of gravity (also radius of curvature) (ft)
- e = Pavement super-elevation (ft/ft)

Equation 4-7 Calculation of side friction (Hall *et al.*, 2009)

It is important to note that the relationship shown in Equation 4-7 does not describe the absolute friction generated but rather describes the relative change in friction arising from changes in the input parameters. This can be demonstrated by resolving the units of the input parameters.

$$\frac{V^2}{15R} - e = \frac{\left(\frac{distance}{time}\right)^2}{distance} - \frac{distance}{distance}$$

Therefore:

$$\frac{\left(\frac{distance}{time}\right)^2}{distance} - \frac{\cancel{distance}}{\cancel{distance}} = \frac{distance^2}{time^2} \times \frac{1}{distance}$$

Therefore:

$$\frac{distance^{\cancel{2}}}{time^2} \times \frac{\cancel{1}}{\cancel{distance}} = \frac{distance}{time^2}$$

Equation 4-8 Resolution of the units of the input parameters to Equation 4-7

The resulting unit is one of acceleration which is related to force when the mass of an object is taken into account. Given that the mass of a vehicle remains the same but the mass of different vehicles may differ, the expression in Equation 4-7 therefore reflects the relative friction reaction force to the input parameters for a single vehicle. A more accurate description would therefore be that described in Equation 4-9 which shows friction being proportional to input parameters rather than equating to it.

$$F_s \propto \frac{V^2}{15R} - e$$

Equation 4-9 The relationship between side force friction, vehicle speed, curvature and super-elevation

Combined manoeuvres

Manoeuvres including braking and cornering simultaneously require the [frictional] force to be shared between both [longitudinal and lateral force] mechanisms, meaning that the interaction of the forces leads to a relation in which as one force increases the other decreases by a proportional amount (Flintsch, et al., 2012).

This relationship is shown in the friction circle, Figure 4-5, which shows that for vehicle operations within the vehicle/road friction limits, the braking and turning forces can vary independently on the condition that their vector sum is less than or equal to the limit of friction, defined by the friction circle or friction ellipse. The vector sum of the two combined forces remains constant (circle) or near constant (ellipse). The shape of the friction ellipse (the limit of friction) is defined by tyre and pavement properties and the friction margin is defined by Equation 4-10.

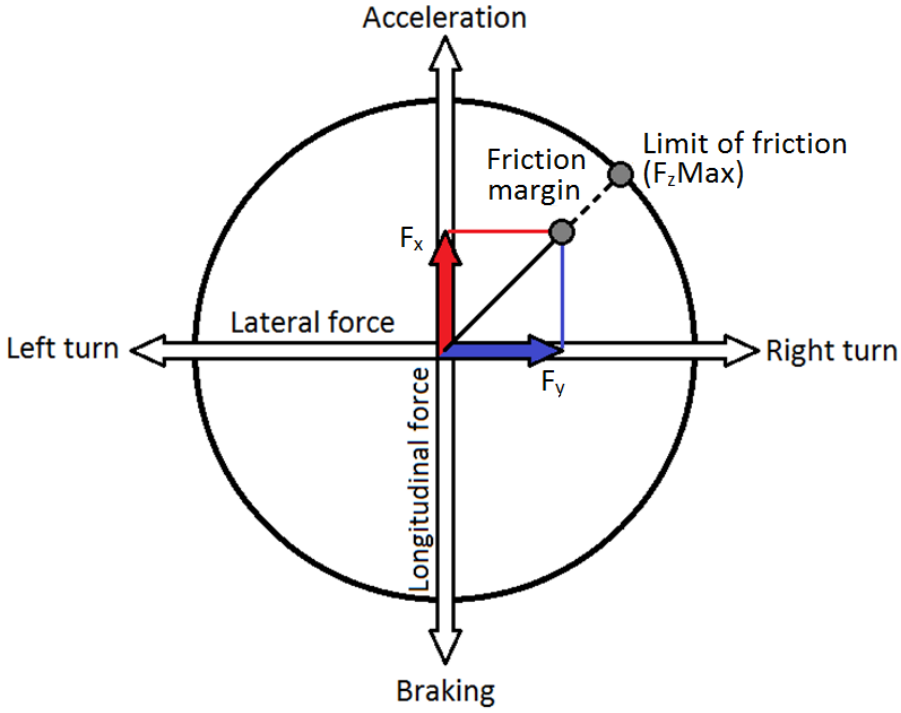

Figure 4-5 Friction circle

$$Friction\ margin = F_zMax - \sqrt{F_x^2 + F_y^2}$$

Equation 4-10 (Singh and Taheri, 2015)

For normal driving conditions, where the frictional forces are not fully demanded, the developing forces will be closer to the centre of the circle. With an increase in friction demand, this will move towards the maximum available friction. Therefore determining the friction coefficient is simpler in high demand conditions than for more normal driving conditions when the tyre slip is smaller. For these situations model-based approaches are

generally being used, which estimate the friction coefficient base on tyre force and moment data (Singh and Taheri, 2015).

4.6 Summary

The main points relevant to this work are:

- Road surface texture depth is a major contributor to friction at high levels of wheel slip, whereas tyre properties and road surface microtexture contribute to the generation of friction at lower levels of wheel slip.
- All of the road friction models assessed used an exponential function to describe the change in friction with wheel slip percentage or vehicle speed.
- Vehicle dynamic control systems (anti-lock braking, traction control, electronic stability control and adaptive cruise control), operate in the region of the friction/slip curve around (at comparable slip ratios to) the peak friction.
- These systems contain proprietary algorithms for estimating the friction available. They make use of vehicle based information such as the longitudinal and lateral motions of the vehicle, wheel speed and steering angle but make relatively crude assumptions about the maximum level of friction available. This is in spite of the many models of tyre/road friction available, which are not regarded as mature and reliable enough to be used within active safety systems.
- Both braking / traction and cornering place a demand on the total friction available from the tyre/road interface. If this is insufficient then the wheel will slide unless countered by one of the active safety systems.

5 Defining the vehicle speed, wheel slip and friction relationship

5.1 Approach

A key task of this work was to develop a methodology capable of characterising the friction performance of road surfacing materials in terms of vehicle speed and wheel slip. The approach taken was to model the performance of individual surfaces as a matrix of values where the position of a value in the matrix described its speed and wheel slip and the magnitude of the value represented the tyre/surface friction. This is illustrated in Figure 5-1, where the matrix is plotted as a three dimensional profile, where the x, y and z axes represent the wheel slip, vehicle speed and friction respectively. This will be referred to as a friction profile.

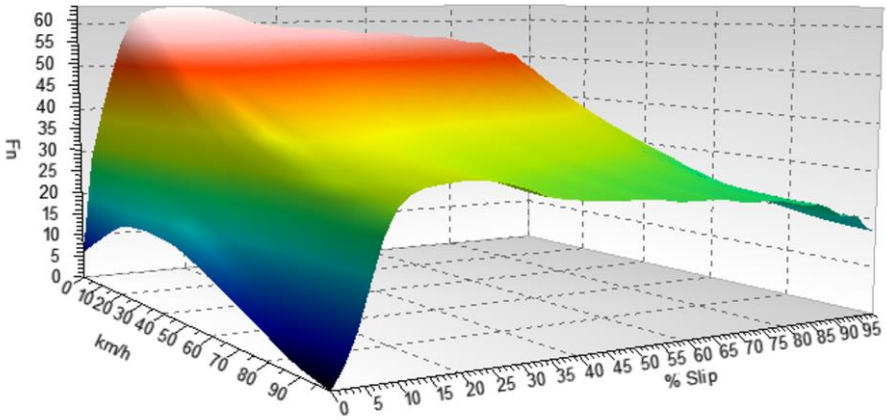

Figure 5-1 Idealised speed (x-axis), slip (y-axis), friction (z-axis) relationship

The matrices were constructed using previous measurements of pavement friction collected using the Highways England locked-wheel Pavement Friction Tester (PFT). Since measurements were collected at different test speeds and were time based, they were combined into a matrix with a consistent spacing in the slip and speed dimensions using the following methodology:

- Collate the individual friction measurements from a surface at different test speeds.
- Perform a linear interpolation on the slip / speed relationship to interpolate data to a resolution of 0.01 units.
- Perform a power regression on the speed, friction relationship to smooth data and interpolate to a resolution of 0.01 units.
- Generate the profile matrices based on the two above interpolations.
- Crop the profile matrices to accept only valid data.

5.2 Collation of friction measurements

Figure 5-2 shows an example of a single locked-wheel measurement. Because the data are collected at fixed time intervals (0.01s) the resulting friction / slip curve (Figure 5-2) has areas where information is highly populated, (60% – 80% slip) or sparse (20% to 30% slip). Furthermore, each measurement is made at a constant test speed (15 km/h in this example). Multiple measurements are made to collect information across the speed range.

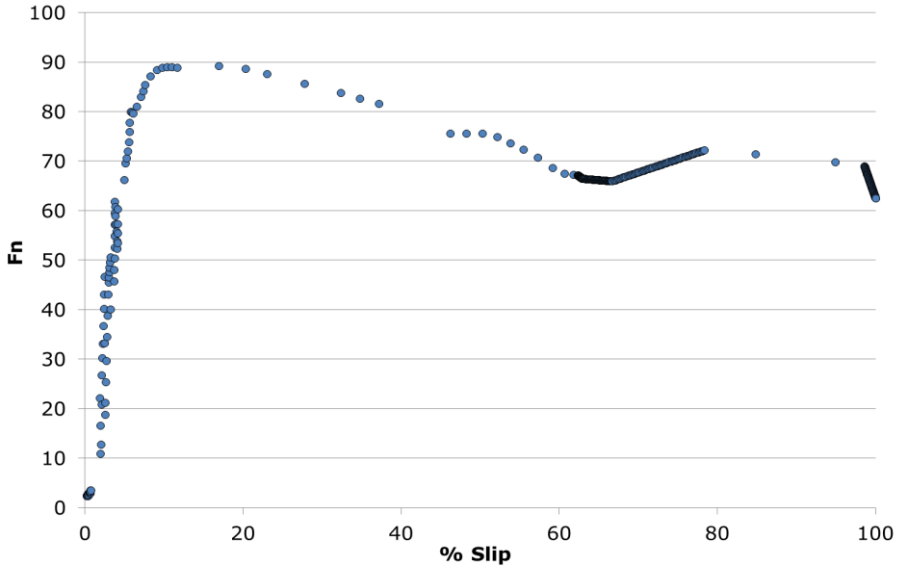

Figure 5-2 Example locked-wheel test

A collection of measurements made on a single surface at different speeds is represented by the data in Figure 5-3. This figure shows how with multiple measurements a 3D profile of the friction performance with respect to vehicle speed and wheel slip can be built.

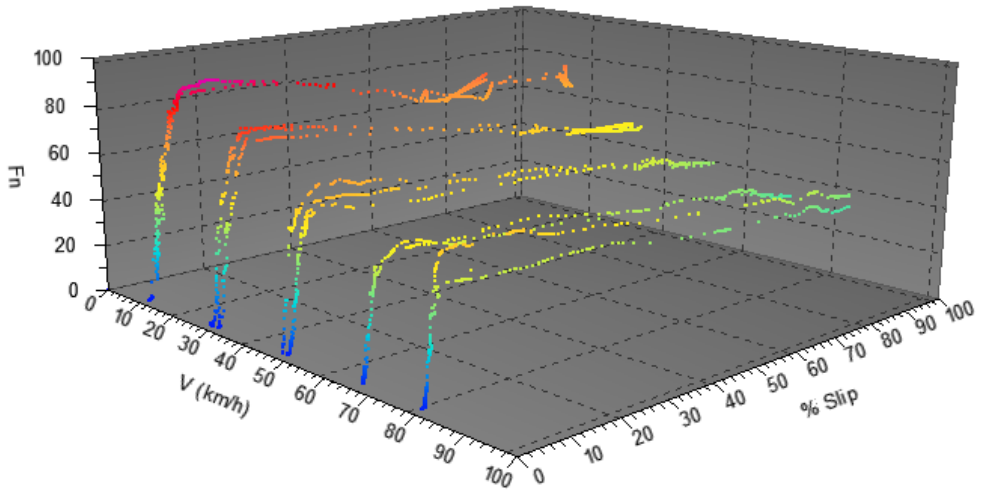

Figure 5-3 Example of measurements made at multiple speeds on a single surface

5.3 Interpolation of the slip/friction relationship

To generate a dense matrix of values describing friction performance, the gaps in Figure 5-3 were filled using interpolation, in two stages. Initially, linear interpolation was used to fill gaps in the % slip/friction direction (x-axis and z-axis respectively), Equation 5-1. This is also shown graphically in Figure 5-4.

$$Fn_x = Fn_0 + \left[(Fn_1 - Fn_0) \times \left(\frac{\%\ Slip_x - \%\ Slip_0}{\%\ Slip_1 - \%\ Slip_0}\right)\right]$$

Where:

- Fn_x = The friction value at % $Slip_x$
- Fn_0 = The closest measured friction value before Fn_x
- Fn_1 = The closest measured friction value after Fn_x
- % $Slip_0$ = The % Slip value at Fn_0
- % $Slip_1$ = The % Slip value at Fn_1

Equation 5-1 Interpolation of friction based on % slip

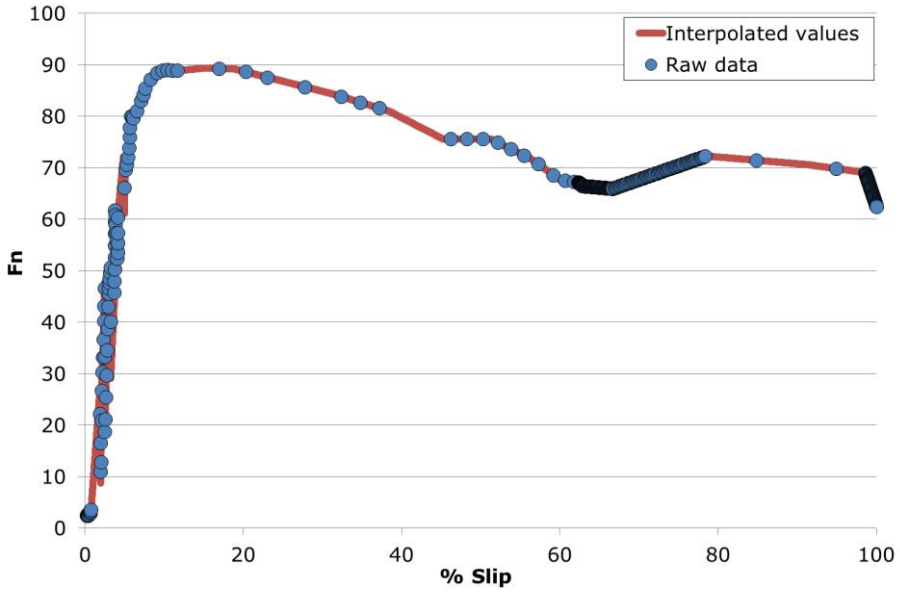

Figure 5-4 Example of interpolation of friction based on % slip

Figure 5-4 shows a typical profile of the % slip and friction relationship recorded using the PFT (the blue series markers) and the interpolated values linking areas where no data were collected (the red line). Below approximately 5% slip the data appear noisy compared to the relatively smooth shape of the rest of the profile. This is because this region contains information from two separate points in the braking cycle, some of these points represent

data collected as the brakes were applied to the test wheel, other points in this area represent data collected as the test wheel was released from its locked state at the end of the test. The points representing post-lockup measurements were included for the following reasons:

- The additional information provided was valuable in assessing the performance of materials at low levels of wheel slip.
- The data from pre and post-lock up provided similar values.
- The amount of interpolation required in this area would be reduced.
- The noise created in the profiles was considered low compared to the overall variation from multiple measurements on the same surface.

5.4 Interpolation of the speed/friction relationship

In the second stage of interpolation, to fill the gaps in measurements between each of the measurement speeds, a model of the friction / speed relationships for each 0.01 % interval on the slip (x) axis was developed. These models were used to populate friction values along the speed (y) axis of Figure 5-3. This also had the effect of smoothing some of the noise that occurs from repeat measurements. An example of this process is shown in Figure 5-5.

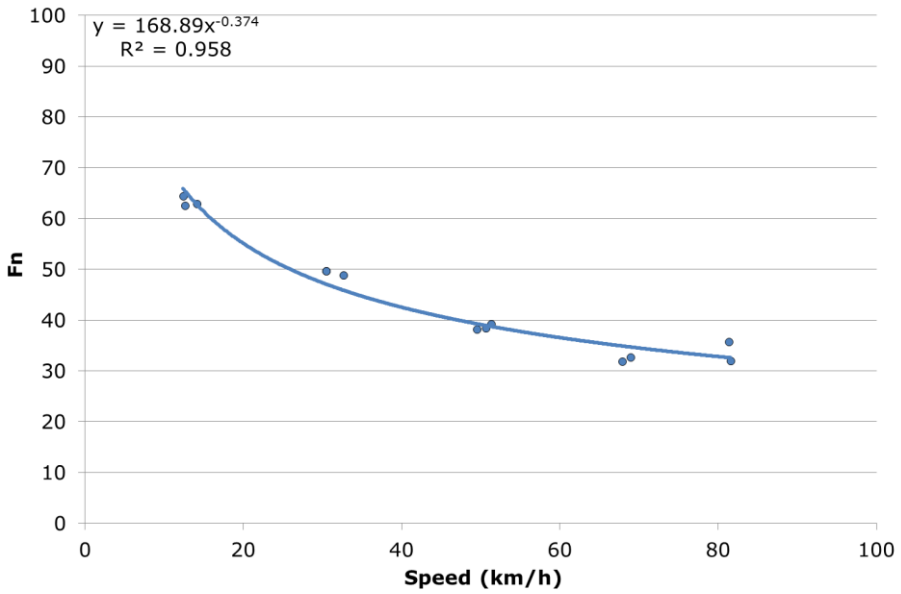

Figure 5-5 Example of interpolation of friction based on vehicle speed

Figure 5-5 shows the speed/friction model for one surface at 100% slip. The relationship between speed and friction for this surface can be described using a power relationship; this was found to be suitable for all the materials tested. Figure 5-5 shows that the use of the power relationship smooths the results and by using the equation describing the relationship, allows friction values at any speed to be interpolated.

5.5 Generation of the friction profile

The interpolation of values allowed a dense matrix of points to be generated describing the friction, speed, slip relationship for individual surfaces. The extent of each matrix was limited as follows:

- Speed ≥ 20 km/h and ≤ 100 km/h, representing the limit of the available data in most cases
- % slip ≥ 2 and ≤ 100, reducing the effect of the noise at very low slip levels from repeat tests on the same surface.

Figure 5-6 is a graphical representation of the matrix generated.

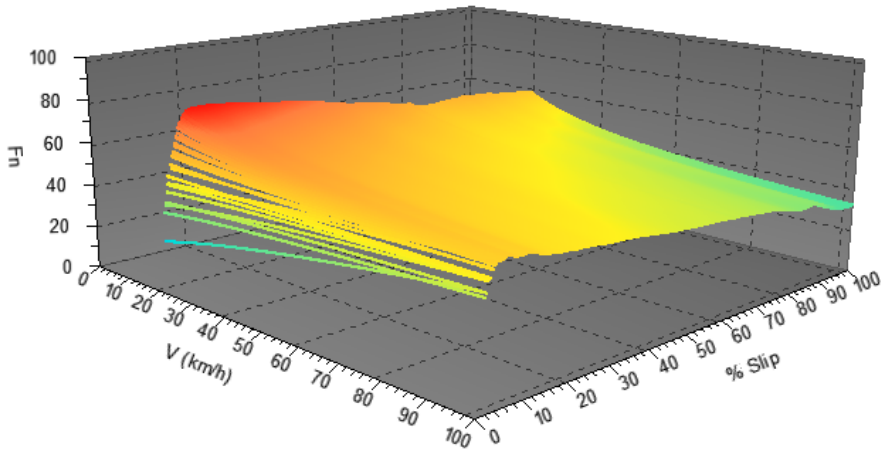

Figure 5-6 Graphical representation of % slip, Vehicle speed, friction matrix

5.6 Verification of profile generation procedure

The approach taken to generate the profiles was validated by defining a minimum requirement for the amount of information used to generate each friction profile, and by comparing the raw data with the generated profiles for a small number of surfaces. The minimum input required measurements made with the PFT at three speeds and three measurements were made per speed. Appendix A provides a summary of the number of individual PFT measurements contributing to each profile.

A comparison between the raw data and that represented by the profiles was carried out by assessing the distribution of the residual values (the profile value minus the measured value) of a small number of profiles generated. The results of this analysis are shown in Figure 5-7 and Table 5-1.

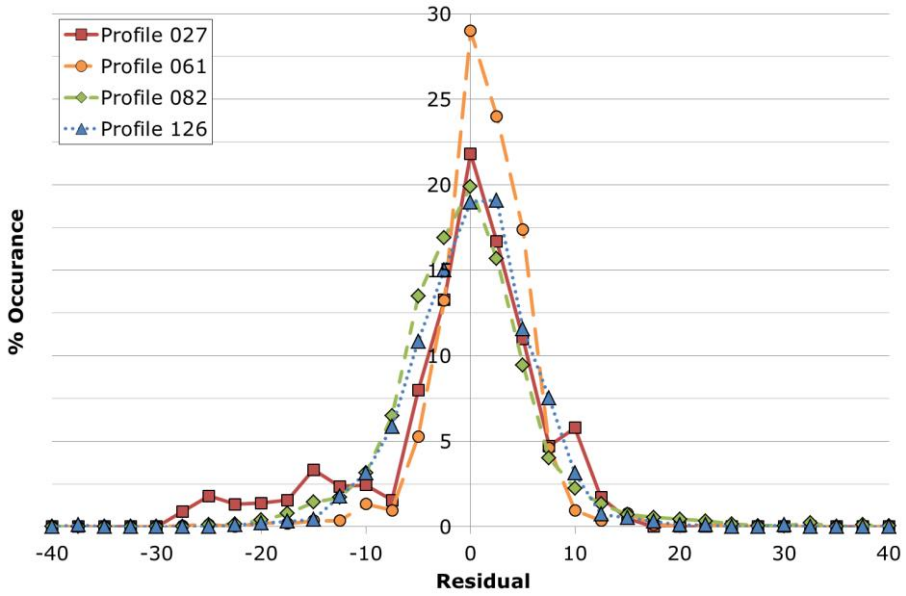

Figure 5-7 Assessment of residual values from profile generation

Table 5-1 Summary of assessed profiles

Profile number	Material	Measurements made	Standard deviation
027	Thin surface course system	15	8.12
061	Brushed concrete	17	4.41
082	Porous asphalt	14	6.77
126	Hot rolled asphalt	15	5.83

Figure 5-7 shows that the distribution of residual values for each profile is normal around zero. The performance of each distribution is similar and although there are variations in the shape of the distributions, these are insubstantial. Table 5-1 shows the standard deviations of the residual values for each profile range between 4.41 and 8.12 inclusive.

The repeatability of the PFT at 100% wheel slip has been identified as between 5.00 and 9.17 inclusive, depending on the speed of the measurement (Brittain and Viner, 2017). The standard deviation of residual values and the repeatability of the PFT are similar and therefore it could be concluded that the methodology used to generate the profiles, closely represents the friction of the surfaces they represent.

6 Assessment of typical material performance

This chapter presents the work carried out to characterise the typical behaviour of different material types.

6.1 Data examined

Friction measurements were made as described by Roe et al. (1998). The dataset used includes data from that original study supplemented by data from later research projects that used the same equipment and equivalent methodology. The data were converted into friction profiles using the methodology detailed in Chapter 5. In total 169 friction profiles were generated for use in this work from 2,494 individual friction measurements made between 1997 and 2013.

To characterise the range of typical performance of each surface type, the friction profiles representing the 5th and 95th percentile of the data were calculated by determining the 5th and 95th percentile of the friction values for individual surfaces within each cell of the slip / speed matrix. In total, data from 113 profiles were used to assess the following material categories:

- Concrete – 41 profiles
- Hot Rolled Asphalt (HRA) – 17 profiles
- Thin Surface Course Systems (TSCS) – 55 profiles combining TSCS materials using the following coarse aggregate sizes:
    - 6 mm – 9 profiles
    - 8 mm – 4 profiles
    - 10 mm – 17 profiles
    - 14 mm – 5 profiles
    - Unknown – 20 profiles

The profiles used in this analysis were identified as having a “normal” relationship between texture and high speed friction.

The results used in this chapter have been further investigated in Chapter 8 to estimate the performance of the surfaces under emergency braking conditions.

6.2 Results

The 5th and 95th percentile profiles for the each material are shown below as 3D plots.

Concrete

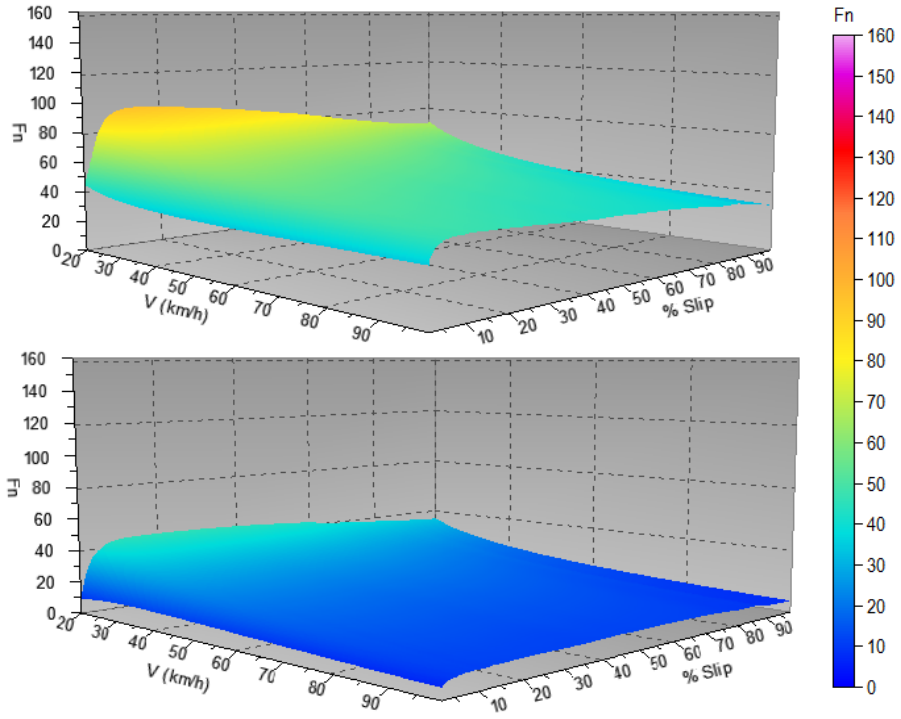

Figure 6-1 5th (below) and 95th (above) percentile profiles for concrete

Hot Rolled Asphalt

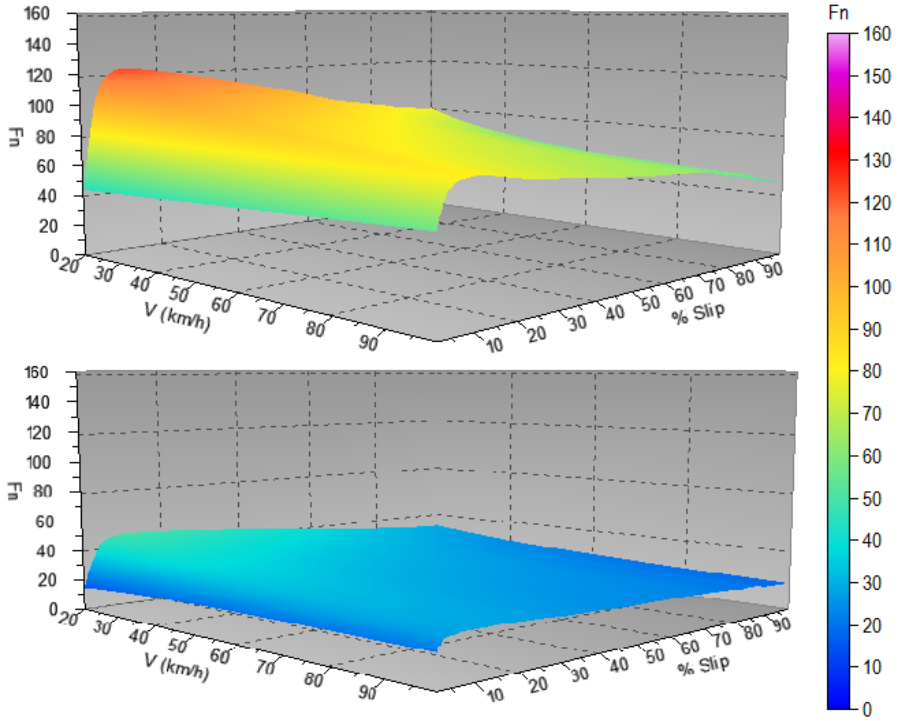

Figure 6-2 5th (below) and 95th (above) percentile profiles for HRA

Thin Surface Course Systems

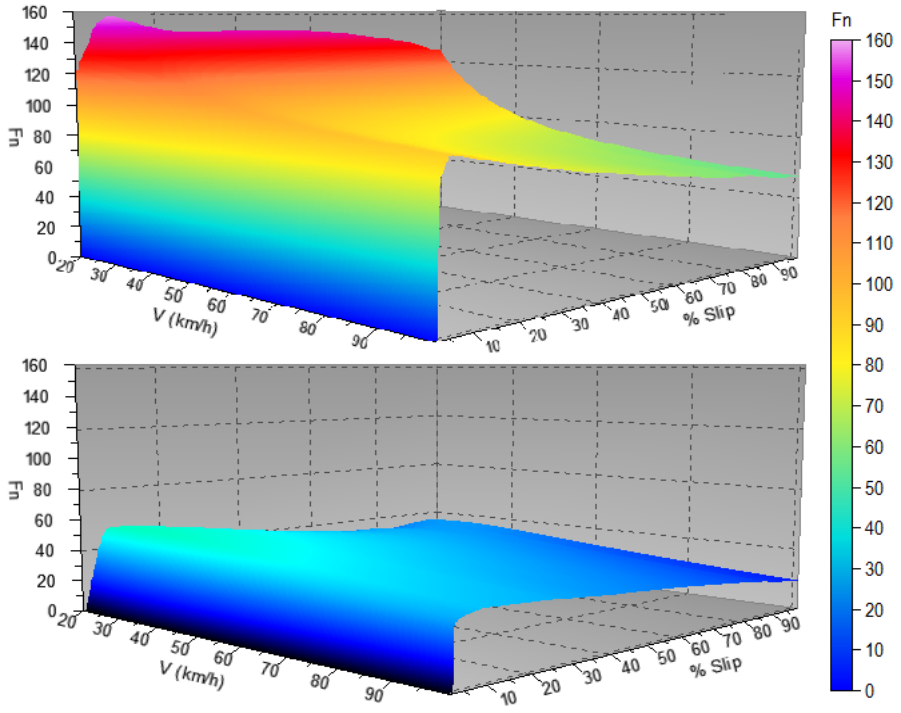

Figure 6-3 5th (below) and 95th (above) percentile profiles for TSCS

6.3 Observations

There is a clear difference in performance between the three materials, the TSCS and concrete materials provide the highest and lowest levels of friction respectively. The 90th percentile range was largest on the TSCS and smallest on the concrete. A low 90th percentile range would be expected on materials with generally low friction properties because there is a greater limitation on the number of possible friction values.

Despite having the greatest friction performance, the 90th percentile range on the TSCS is nevertheless high. An explanation for this could be that this material includes within it multiple sub-divisions of materials that have a wide ranging performance. Unfortunately it was not possible to conduct a similar analysis on these sub-divided materials as there was a limited amount of information available.

7 Development of a friction prediction model

Building on the friction profile matrices developed in Chapter 6, a generic model was developed to predict the friction profile of a surface from measurements of low speed skid resistance and texture depth; referred to as the friction model.

These variables were selected because:

- These were the variables used in previous works to model high speed, locked-wheel friction, reported in TRL367 (Roe *et al.*, 1998), so a direct comparison with this work was possible.
- These parameters are routinely measured on the English SRN as part of the Highways England pavement assessment policy.
- Historical work reported in TRL622 (Parry and Viner, 2005) has shown these parameters to be key indicators of collision risk in certain scenarios.

This section describes how the model was built and validated. In Chapter 8, the friction model is used to assess the significance of low speed friction and texture depth for a vehicle braking manoeuvre.

7.1 Development of the model

The model was built using the multiple linear regression method, in which the overall response (the predicted friction) is modelled as the sum of contributions from variables that are linearly related to the predicted friction. The approach taken can be summarised as:

1. Define assumptions and limitations,
2. Collate data on which the model will be built,
3. Transform the data to produce a linear relationship with friction,
4. Test variables for co-linearity,
5. Perform the regression analysis and define the model.

7.1.1 Assumptions and limitations

The following assumptions and limitations were used for the development of the friction model:

- The model would be based on surfaces with adequate data and displaying a “normal” relationship between texture and high speed friction[A].
- Thereafter, all material types can be modelled together.
- The inputs would be texture depth (SMTD) and low speed skid resistance (SC(50)); it is assumed the variation in friction can be described by these two variables.

[A] To remove surfaces showing effects unexplained by the input variables of the model (see section 7.1.2)

- The limitations of the valid output are 2 – 100 % slip and 20 – 100 km/h speed.

7.1.2 Collation of dataset for modelling

The friction model was built using matrices describing individual surfaces developed in Section 5.5 instead of the raw PFT measurements. The reason for doing so is justified because these matrices are simply mathematical descriptions of the raw measurements that would otherwise be carried out as part of the modelling methodology.

Data from sixteen of the surfaces were removed from the dataset on which the model was built because it was clear from the relationships between texture and high speed friction that a factor other than those used in the model was having a considerable effect on the friction value. This is demonstrated in Figure 7-1 which shows the relationship between texture and locked-wheel friction at 100 km/h (L-Fn100) for the dataset. The points within the red circle represent materials that have been identified as having a substantial contributing factor that would not be captured by the model. Research into the possible factors that contribute to this increase in friction performance is provided in TRL Report PPR727 (Sanders *et al.*, 2014).

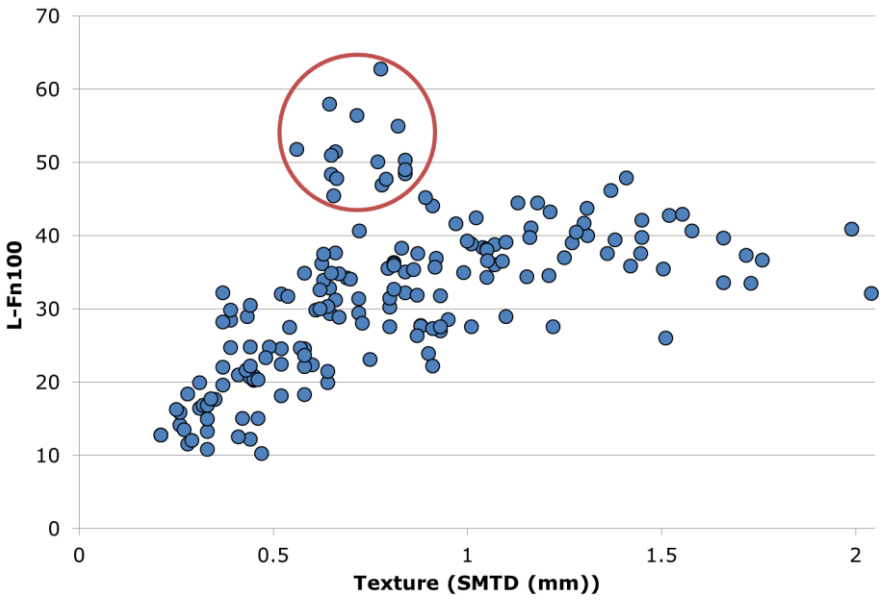

Figure 7-1 Texture and high speed friction relationships

The following information was then collated from all of the remaining friction profiles:

- Profile number
- % slip in 1% increments
- Vehicle speed in 1 km/h increments
- Texture depth (SMTD) associated with the profile number
- Low speed skid resistance (SC(50)) associated with the profile number

- Friction value associated with the % slip / Vehicle speed combination gained from the matrix associated with the profile number

This resulted in a dataset of 6 columns by 1,143,072 rows as per the example in Table 7-1.

Table 7-1 Example of the reference dataset used to develop the model

Profile number	% Slip	Speed (km/h)	SMTD (mm)	SC(50)	Fn
027	2	20	0.52	0.51	22.09
027	3	20	0.52	0.51	48.07
…	…	…	…	…	…
263	100	100	0.81	0.56	35.94

7.1.3 Variable transformations

The multiple linear regression analysis method requires the input variables (% slip, vehicle speed, low speed skid resistance and texture depth) to correlate linearly with the predicted variable (friction). In cases where the input variables do not linearly correlate with the predicted variable, it is sometimes possible to carry out a mathematical operation on the input variable to obtain a linear correlation, this is known as a transformation.

Figure 7-2 to Figure 7-5 show the relationships between each input variable and friction, displayed by the blue series. In cases where these do not correlate linearly with friction the transformation required to obtain a linear correlation is shown, the red series.

Figure 7-2 shows the relationship between texture and friction for one vehicle speed, the line of best fit for the relationships is a logarithmic relationship ($y = a \times \log(x) + b$) with a coefficient of determination (R^2 value) of 0.67. Applying a logarithmic transformation to the texture variable results in a linear correlation between the natural logarithm of texture and friction.

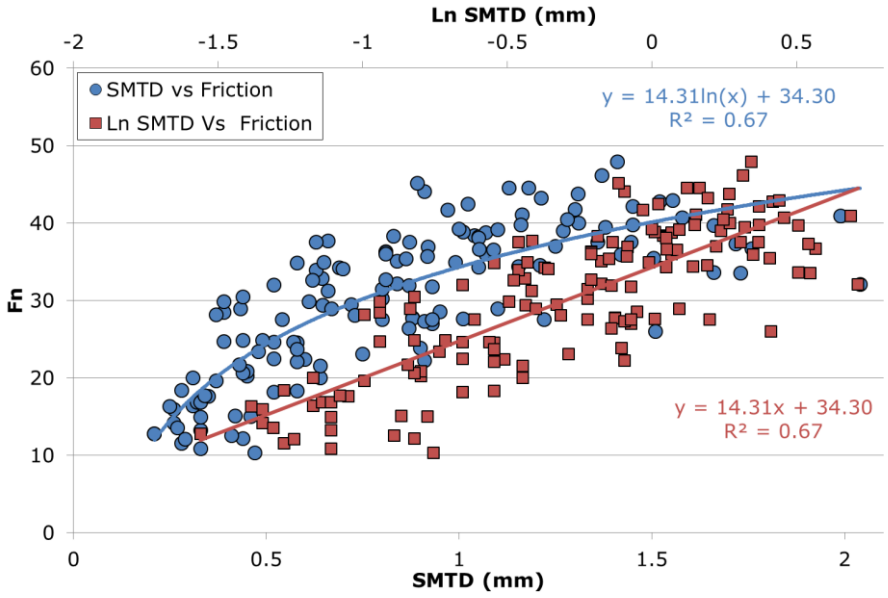

Figure 7-2 Texture and friction relationship

Figure 7-3 shows the typical relationship between vehicle speed and friction for one material, as expected the line of best fit is a power relationship ($y = ax^b$) with an R^2 value of 1. This is expected because this relationship has already been modelled as part of the procedure for generating the matrices from which these data were obtained. Applying a double logarithmic transformation to the speed variable results in a linear correlation between the natural logarithm of the natural logarithm of the speed and friction.

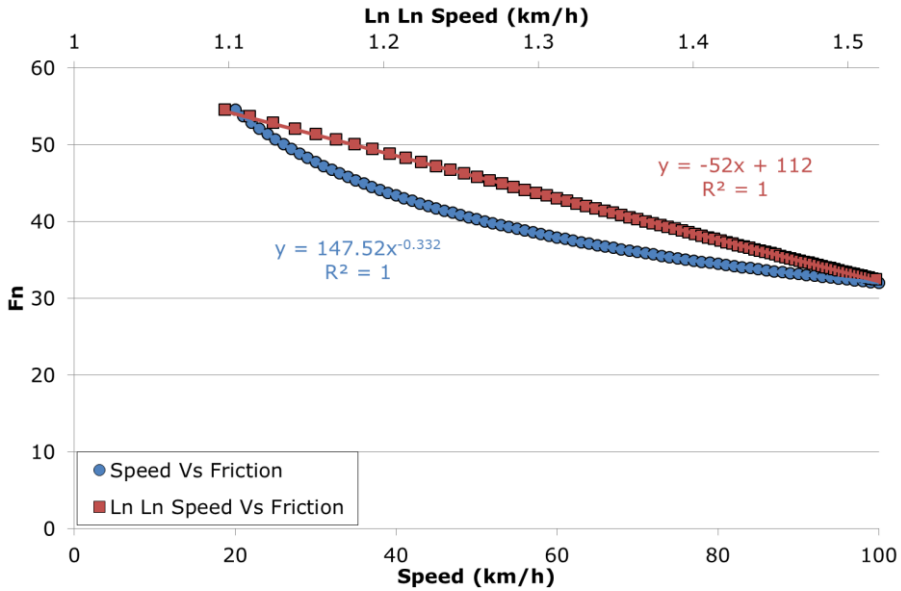

Figure 7-3 Vehicle speed and friction relationship

Figure 7-4 shows the relationship between low speed skid resistance and friction measured at 100% slip and 20km/h, the line of best fit is a linear relationship ($y = m \times x + c$) with an R^2 value of 0.29. As this relationship is already approximately linear, no transformation is required.

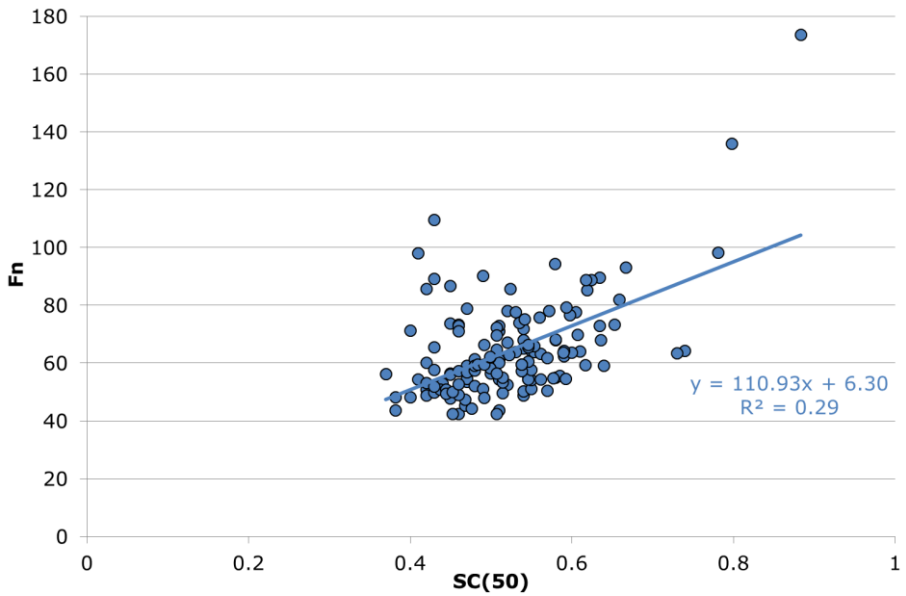

Figure 7-4 Low speed skid resistance and friction relationship

Figure 7-5 shows the relationship between % slip and friction for one material. The line of best fit is a linear relationship ($y = m \times x + c$) with an R^2 value of 0.87. However the use of this relationship is undesirable in the context of this work as doing so would have the potential to inaccurately model the extremes of behaviour. Within the context of this research it is the extremes of behaviour, particularly the very low and very high % slip values that are of interest.

It was therefore decided to remove the % slip variable from the model and instead to model the behaviour at each % slip interval separately. This would create a large table describing the relationship between low speed skid resistance, texture and vehicle speed at each percentage slip interval. This approach was considered preferable to including % slip in the model which would lead to a potentially inaccurate output at the extremes of % slip.

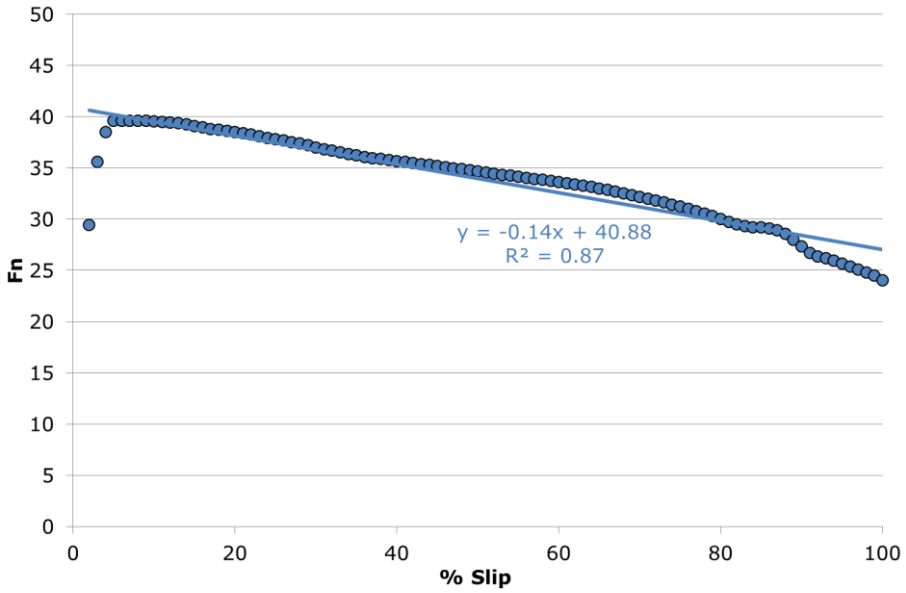

Figure 7-5 % Slip and friction relationship for the reference data

7.1.4 Assessment of collinearity

An assessment of collinearity was carried out to ascertain if any of the input variables were linearly correlated to any of the other input variables. The linear correlation of input variables is undesirable when using the multiple linear regression technique as this can lead to errors occurring in the model predictions.

The assessment of collinearity was carried out by plotting the relationships between all of the input variables separately and analysing the statistics of a linear trend line. Figure 7-6 to Figure 7-8 show the relationships between pairs of the input variables. In each figure the blue series markers represent the variable values, the red line represents the linear trend line and the red text gives the equation of the trend line and the R^2 value. The lower the amount of linear correlation between the two variables assessed the lower the gradient of the trend line and the smaller the R^2 value.

Figure 7-6 and Figure 7-8 show no linear correlation between Ln Ln speed and Ln SMTD, and, SC(50) respectively. Figure 7-7 shows that the linear trend line between Ln SMTD and SC(50) has a gradient of 0.02 and a R^2 value of 0.02. These values are markedly greater than those observed with the other relationships, but not so great as to indicate a collinearity.

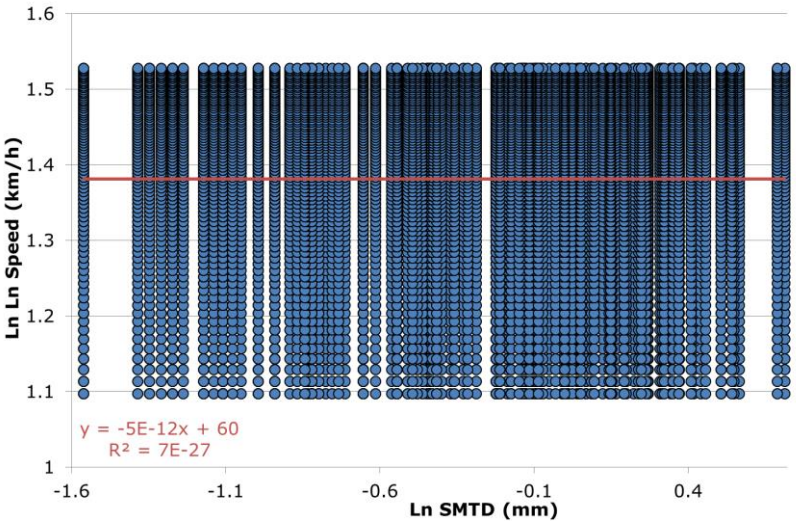

Figure 7-6 Relationship between Ln SMTD and Ln Ln Speed

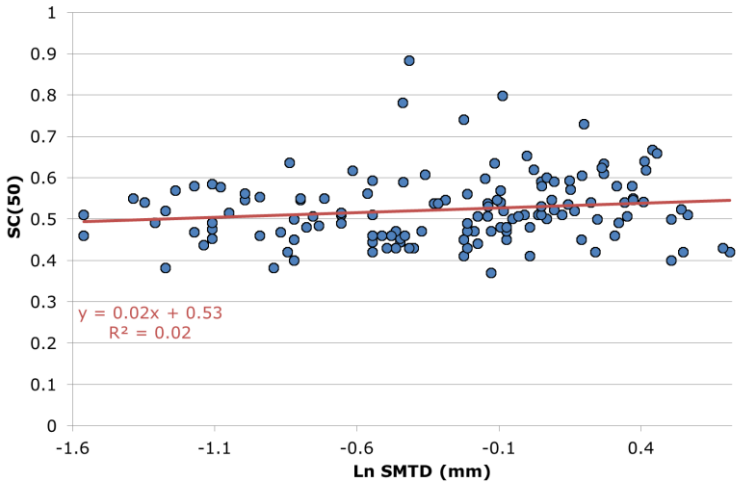

Figure 7-7 Relationship between Ln SMTD and SC(50)

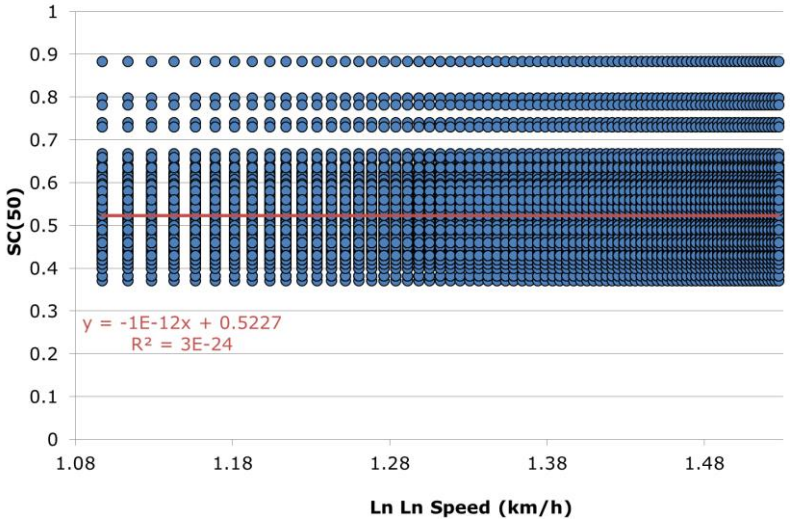

Figure 7-8 Relationship between Ln Ln Speed and SC(50)

7.1.5 Linear regression analysis and model description

Table 7-2 is an example of the dataset on which the regression analysis was carried out; a separate table was produced for each % slip interval. A multiple linear regression analysis was then carried out on each of the tables using the "Regression" tool in Microsoft Excel.

Table 7-2 Example of model variables used

Dependant variable	Independent variables		
Fn	Ln Ln Speed (km/h)	Ln SMTD (mm)	SC(50)
22.09	1.097	-0.65	0.51
48.07	1.097	-0.54	0.51
…	…	…	…
35.94	1.527	-0.21	0.56

The results from the regression analysis allowed the model to be described using Equation 7-1. The model coefficients for each % slip interval are provided in Appendix B.

$$Fn_x = a_x + \left[b_x \times Ln\left(Ln(Speed)\right)\right] + \left[c_x \times Ln(SMTD)\right] + \left[d_x \times SC(50)\right]$$

Where:

- Fn_x = the friction value at a given % Slip x
- a_x = the model coefficient at % Slip x
- b_x = the speed coefficient at % Slip x
- c_x = the texture coefficient at % Slip x
- d_x = the low speed skid resistance coefficient at % Slip x

Equation 7-1 Description of the friction model

7.2 Model validation

The model predictions were compared with the original, raw friction measurements. (This approach limited the amount of raw data available as the friction model was limited to calculating friction values at integer values of % slip. Corresponding raw measurements comparisons could only therefore be carried out on integer values of % slip. Despite this limitation, 122,018 values were calculated which was considered adequate for validating the model performance.)

Figure 7-9 shows the relationship between the predicted and actual friction values. The relationship is largely linear but a small cluster of values are present below the main cluster, highlighted by the red boundary. A manual assessment of a sample of these points indicated that they have a tendency to be generated at very low values of wheel slip.

This is demonstrated in Figure 7-10 which excludes values relating to a wheel slip below 5%. It can be seen that the majority of values within the red area have been removed.

The line of best fit describing the relationship between predicted and measured friction values, Figure 7-9, is linear with a gradient of 0.98 and an R^2 value of 0.67. These values are encouraging as they indicate a strong relationship between the predicted and actual values.

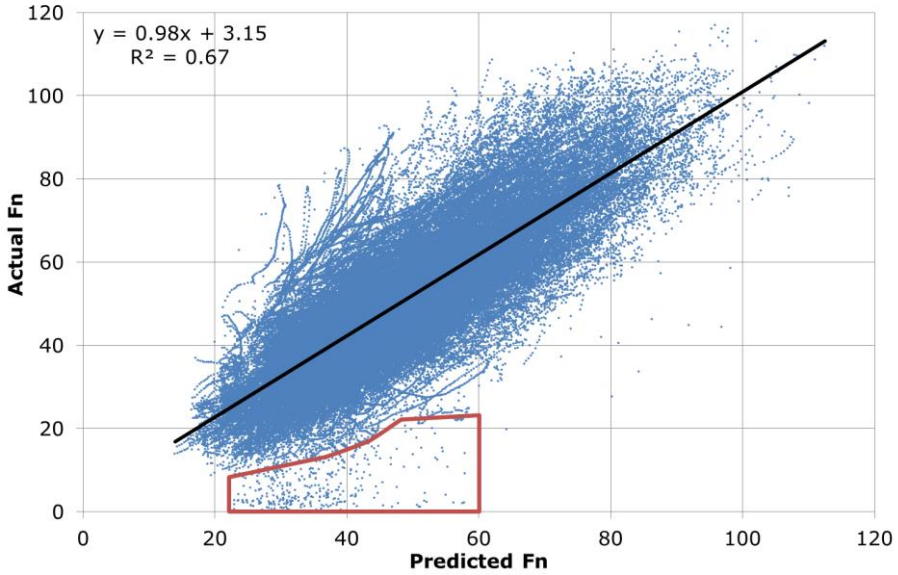

Figure 7-9 Predicted vs. measured friction values

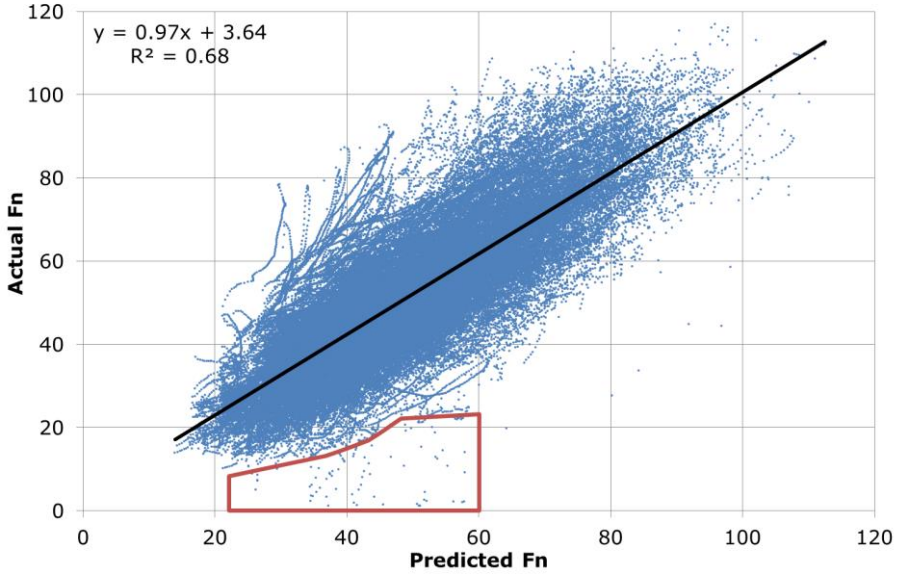

Figure 7-10 Predicted vs. measured friction values, excluding data < 5% slip

The distribution of the residual values (observed friction minus predicted friction) was used to assess the model accuracy. Figure 7-11 shows the distribution of the residual values and the 1, 2 and 3 standard deviation ranges (the red chequered, blue cross hatch and green lined areas respectively). The distribution of residuals forms a bell curve with a mean value of zero. The 1, 2 and 3 standard deviation ranges represent the 68%, 95% and 99.7% likelihood of the residual of any value falling within the ranges indicated by the x-axis. In this case there is a 68%, 95% and 99.7% likelihood that the friction prediction will fall within approximately 10, 20 and 30 units respectively of the actual friction value.

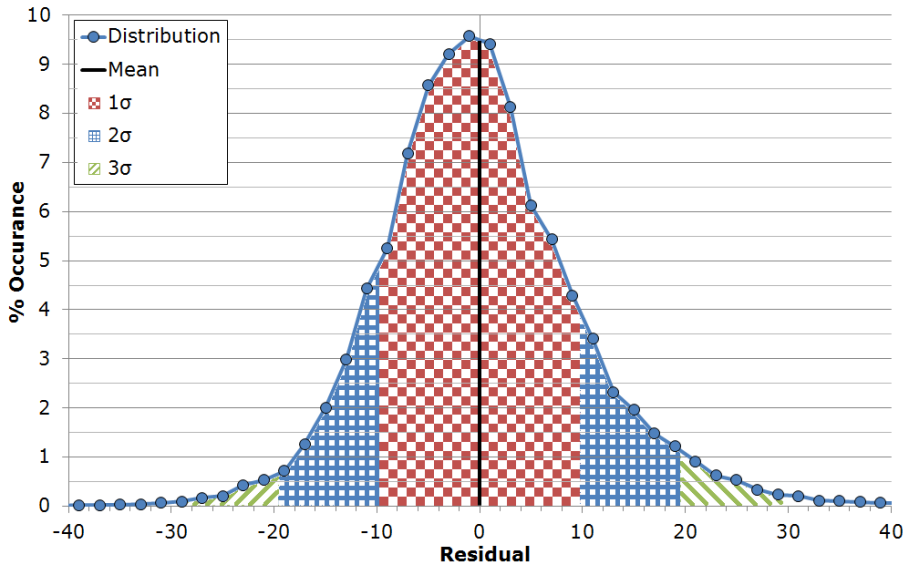

Figure 7-11 Distribution of residual values

To add context to this analysis, a comparative analysis was conducted on the TRL367 model. This consisted of calculating the distribution of the residual values generated by the TRL367 model on the data used to build that model (Roe *et al.*, 1998); the results of this analysis are shown in Figure 7-12. The distribution of residuals of the TRL367 values has 1, 2 and 3 standard deviation ranges of approximately 6, 12 and 18 units. The accuracy of the TRL367 model is therefore greater than that of the friction model. However the TRL367 model is limited to estimating friction at one vehicle speed and one slip speed only.

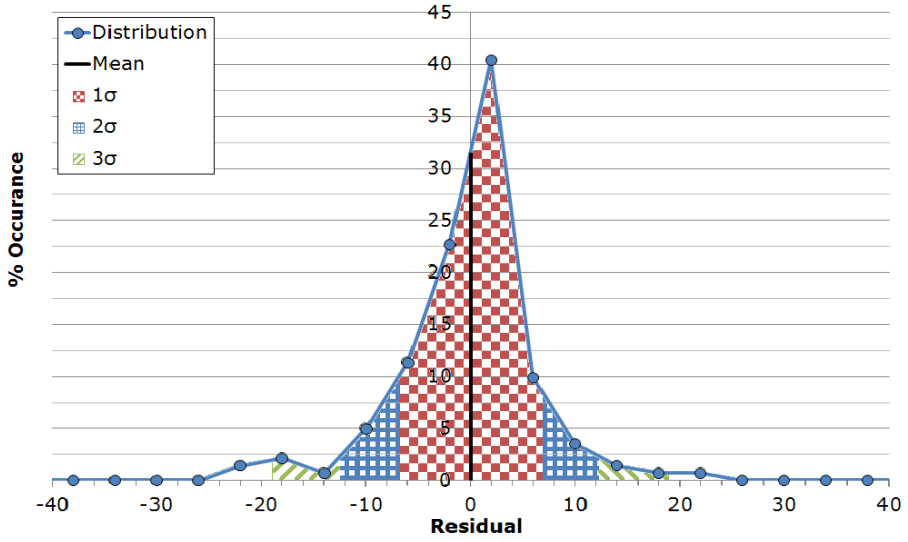

Figure 7-12 Distribution of residual values for model reported in TRL367

A more detailed analysis of the residual values from the friction model was carried out to assess the accuracy of the model for different input variables. The distributions of residual values corresponding to different % slip values are shown in Figure 7-13. This shows that for % slip values greater than 2% the distribution follows closely that of the distribution of

all values. The distribution of values corresponding to very low % slip show a higher propensity to produce lower residuals, indicating that the model has predicted a higher friction value than the value measured. This finding is in line with the observations associated with the highlighted area in Figure 7-9.

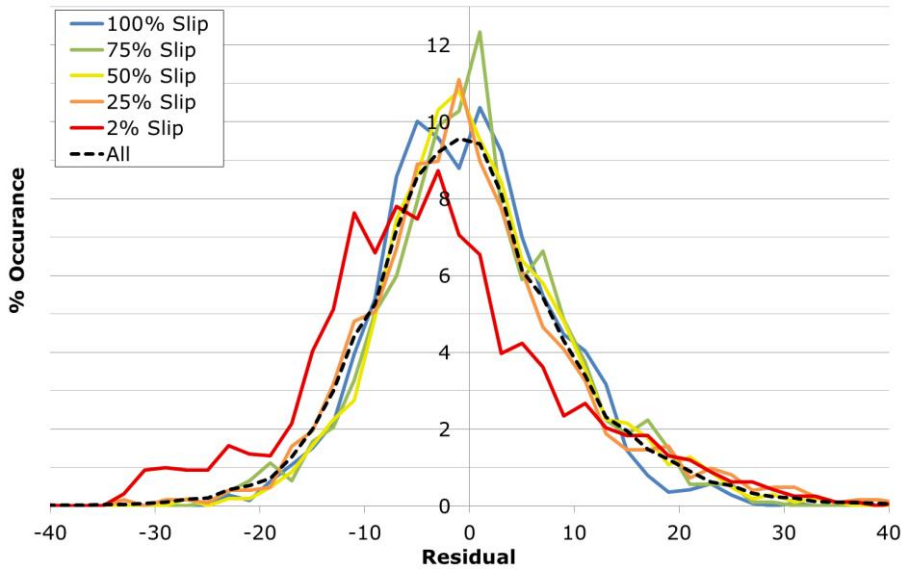

Figure 7-13 Distribution of residual values for different % slip values

The distributions of residual values corresponding to different vehicle speeds are shown in Figure 7-14. The distributions follow a bell curve shape but with different amounts of skew for each vehicle speed. At 50 and 80 km/h there is a slight skew to the right of the mean and at 30 km/h there is a skew to the left of the mean. This suggests the vehicle speed element in the model does not fully represent the effect of speed. However, the level of inaccuracy is relatively small.

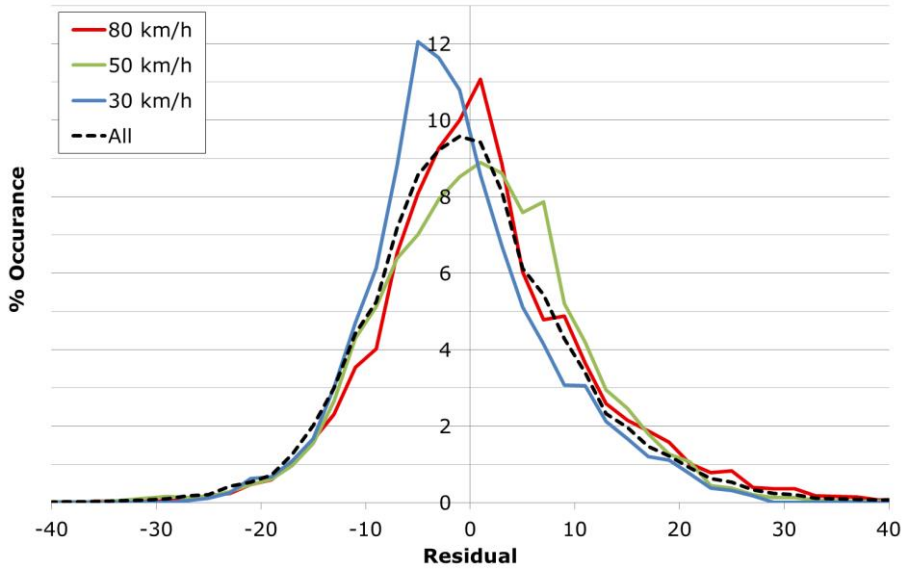

Figure 7-14 Distribution of residual values for different vehicle speeds

The distributions of residual values corresponding to different levels of low speed skid resistance are shown in Figure 7-15. These distributions show a pattern of changing skew of the distribution from positive to negative with increasing low speed skid resistance. The most extreme case is observed at the lowest SC(50) values where the mean of the distribution is approximately 5 units. This indicates that the model is over-predicting the friction properties for materials with very low SC(50) values and, to a lesser extent, under-predicting the friction properties for materials with high SC(50). The over-prediction of values with low SC(50) values is fail-unsafe and so there may be justification for limiting the use of the model for surfaces with low SC(50) values in practice.

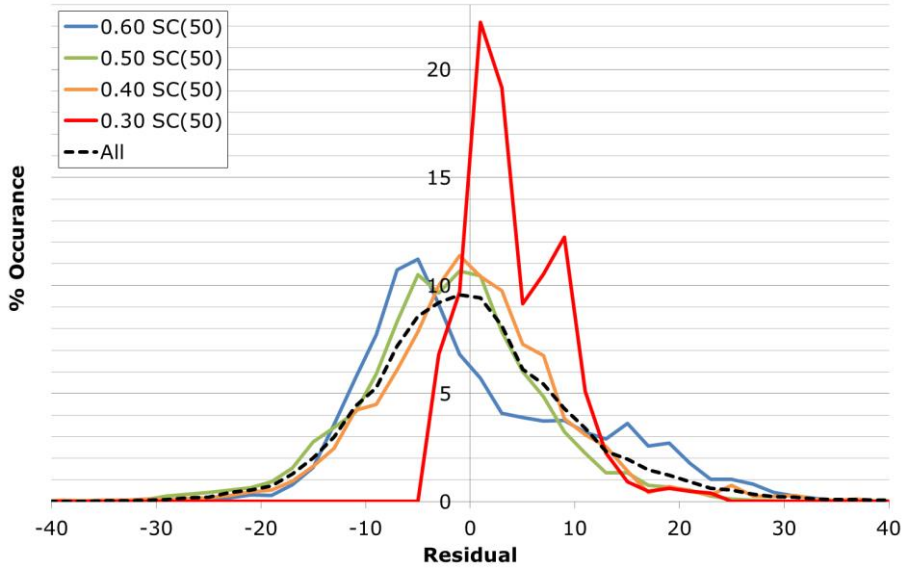

Figure 7-15 Distribution of residual values for different values of low speed skid resistance

7.3 Observations from friction model validation

The following key observations were made from the model validation exercise:

- No colinearity was observed between any of the input variables.
- On average, the model explains nearly 70% of the variation in the observed friction values.
- A small number of input values corresponding to very low values of wheel slip are not predicted well by the model.
- Analysis of the residual values has shown that there is a 68%, 95% and 99.7% likelihood that a residual measurement will fall within approximately 10, 20 and 30 units respectively of the actual friction value.
- The model may over-predict the performance of materials with very low values of SC(50). Otherwise, there is little evidence for systematic bias within the model predictions.
- The friction model is less accurate than the TRL367 model, but is capable of estimating friction across a larger rage of vehicle speeds and wheel slip percentages, whereas the TRL367 model estimates friction at a single vehicle speed and wheel slip percentage.

8 Significance of low speed skid resistance and texture on vehicle manoeuvres

Having, in Chapter 7, developed a friction model to describe the shape of the friction / speed / slip profile seen in Figure 5-1, this section investigates the implications of the shape of the friction profile for an example manoeuvre, vehicle braking.

The performance of surfaces with various nominal levels of low speed skid resistance and texture depth were compared by calculating the distance required for a vehicle to reduce its speed from a specified initial speed to 20 km/h, under emergency braking, with and without ABS. The model built to carry out this analysis will be referred to as the braking model.

8.1 Braking model methodology

The process for developing the braking model can be summarised as:

1. Define assumptions and limitations.
2. Define a method to estimate the time taken to reach peak and locked-wheel friction on surfaces with varying friction characteristics.
3. Specify the initial conditions to be input for each model.
4. Define the iteration process to estimate the braking time and distance.

8.1.1 Definition of assumptions and limitations

The braking model uses an iterative process in which the predicted friction, for the given vehicle speed and wheel slip, is used to determine the instantaneous deceleration and distance travelled within each step of the iteration. The following assumptions and limitations were used for the development of the braking model:

- The deceleration of the vehicle can be characterised by the friction available for braking, defined by the friction model from Chapter 7. This assumes the braking performance of the vehicle is represented by the smooth tyre friction with a 1 mm water film thickness, as used in the original measurements.
- The use of ABS will hold the friction value at the peak friction value.
- The % slip / Speed relationship for the PFT is linear. This is justified in section 8.1.2
- Vehicle speeds below 20 km/h are not considered due to lack of data limiting the extent of validity of the friction model.

8.1.2 Estimate time to reach peak and locked-wheel friction

An estimate of the wheel slip occurring during each iteration is needed to determine the predicted friction level. This was estimated from existing locked-wheel skid test data, by analysing the time taken for the test wheel to reach its peak and locked-wheel states.

Figure 8-1 and Figure 8-2 plot the time taken to achieve locked-wheel and peak friction respectively in each of the individual measurements making up the database used to derive the friction model. These show that the time taken to achieve locked-wheel and peak

friction depends on the friction of the surface measured and the initial speed of the vehicle. A multiple linear regression was carried out on the vehicle speed and friction variables to produce equations that predict the time taken to achieve locked-wheel and peak friction (Equation 8-1 and Equation 8-2). These equations were used to predict the time taken to achieve locked-wheel and peak friction based on the initial conditions of the braking model.

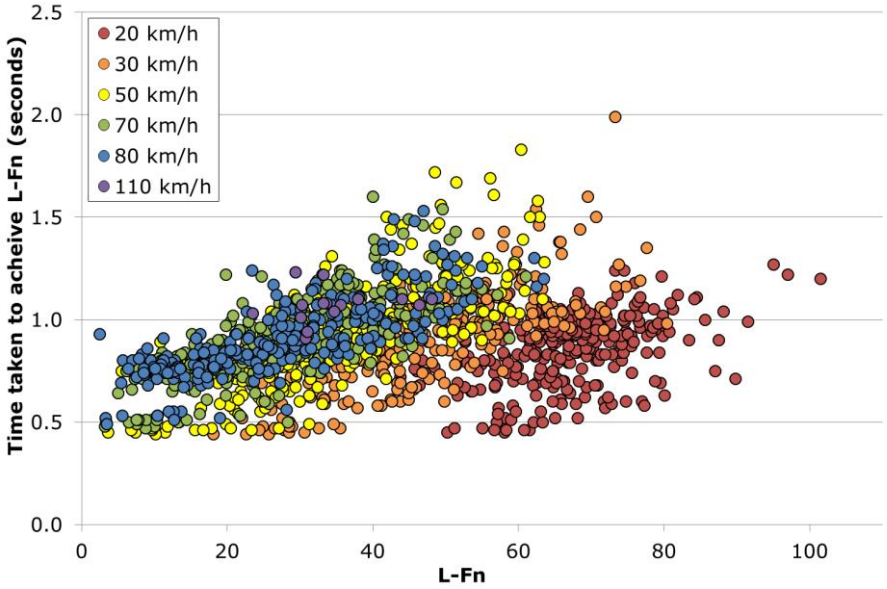

Figure 8-1 Relationship between vehicle speed, locked-wheel friction and the time taken to achieve locked-wheel friction

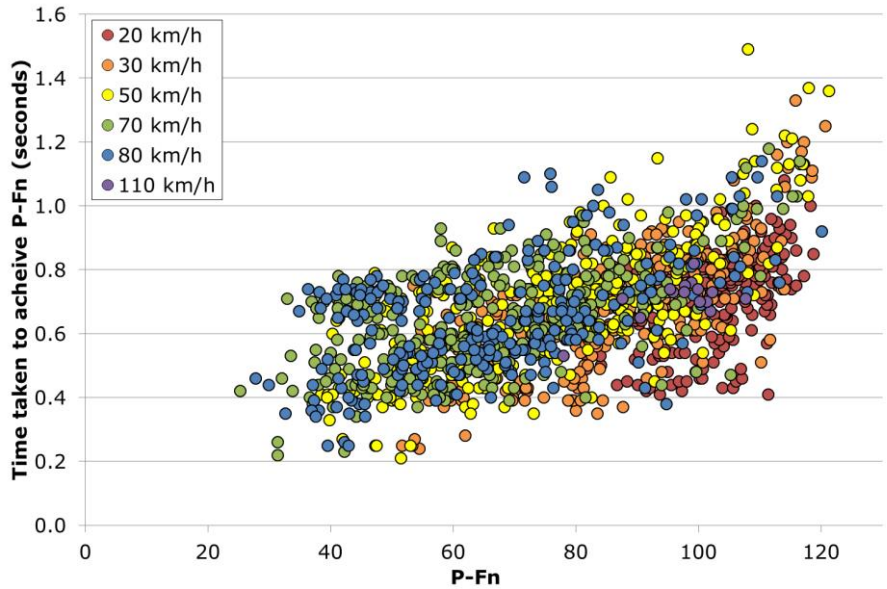

Figure 8-2 Relationship between vehicle speed, peak friction and the time taken to achieve peak friction

$$t_L = 0.140732 + (0.001966 \times S) + (0.005392 \times LFnS)$$

Where:

- t_L = the time taken to achieve locked-wheel friction (seconds)
- S = the average speed of the measurement (km/h)
- LFnS = the locked-wheel friction of the surface at speed S

Equation 8-1 Estimation of the time taken to achieve locked-wheel friction

$$t_P = 0.140732 + (0.001966 \times S) + (0.005392 \times PFnS)$$

Where:

- t_P = the time taken to achieve peak friction (seconds)
- S = the average speed of the measurement (km/h)
- PFnS = the peak friction of the surface at speed S

Equation 8-2 Estimation of the time taken to achieve peak friction

8.1.3 Specify the initial conditions for the model

The input conditions required for each model are:

- Initial vehicle speeds (V1) of 50, 75 and 100 km/h were modelled in order to assess the influence of vehicle speed.
- Initial % slip. Set to 2% in all cases, which is the lower limit of the friction model.
- SMTD. Varied between 0.2 and 2.0 to determine the influence of texture depth.
- SC(50). Varied between 0.20 and 0.60 to determine the influence of low speed skid resistance.
- ABS Used. Set to "Yes" or "No" to assess the performance with and without the use of driver aids.

8.1.4 Define the iteration process used to estimate the braking time and distance

Starting from the initial conditions, the braking model calculates: the % slip, the vehicle acceleration (from the friction model, given the % slip and the vehicle speed), and the change in vehicle speed and the distance travelled during each iteration. This is continued through iterations of 0.01s until the speed of the vehicle reaches 20 km/h.

% Slip

The % slip of the wheels was derived using the times taken to achieve locked-wheel and peak friction to limit the linear relationships between % slip and time. Equation 8-1 and Equation 8-2 were used to estimate the time taken to achieve peak and locked-wheel friction in the prediction model by exchanging the "S" term in each equation with "V_1". The LFnS and PFnS terms in each equation were then estimated using the friction model.

The values gained were used to estimate the amount of slip experienced at each time interval using linear interpolation, as given in Equation 8-3 to Equation 8-7.

In the case where ABS is not used the following equations are used:

$$\%\ Slip_t = \underset{t \le t_P}{^{t \ge 0}}\left[\%\ Slip_0 + \left((\%\ Slip_P - \%\ Slip_0) \times \frac{t}{t_P}\right)\right]$$

Where:

- t = time since brake activation (seconds)
- % $Slip_t$ = The percentage slip estimated at time "t"
- % $Slip_0$ = The percentage slip at time = 0 (this is always 2, given the model restrictions)
- % $Slip_P$ = The percentage slip at peak friction

Equation 8-3 Estimation of the % Slip at any given time before peak friction is achieved and ABS is not used

$$\%\ Slip_t = \underset{t \le t_L}{^{t > t_P}}\left[\%\ Slip_P + \left((100 - \%\ Slip_P) \times \frac{t - t_P}{t_L - t_P}\right)\right]$$

Equation 8-4 Estimation of the % Slip at any given time after peak friction is achieved and ABS is not used

$$\%\ Slip_t = \underset{t=\infty}{^{t > t_L}}[\%\ Slip_L] = 100$$

Equation 8-5 Estimation of the % Slip at any given time after locked-wheel friction is achieved and ABS is not used

In the case where ABS is used the following equations are used:

$$\%\ Slip_t = \underset{t \le t_P}{^{t \ge 0}}\left[\%\ Slip_0 + \left((\%\ Slip_P - \%\ Slip_0) \times \frac{t}{t_P}\right)\right]$$

Equation 8-6 Estimation of the % Slip at any given time before peak friction is achieved and ABS is used

$$\%\ Slip_t = \underset{t=\infty}{^{t > t_P}}[\%\ Slip_P]$$

Equation 8-7 Estimation of the % Slip at any given time after peak friction is achieved and ABS is used

Speed

The vehicle speed throughout the braking cycle was calculated on an iterative basis by using the acceleration experienced during the previous time interval to calculate the speed at the next (Equation 8-8 and Equation 8-9).

$$a = (Fn \times 9.806)/100$$

Where:

a = the acceleration experienced by the vehicle (m/s^2)

Fn = the friction predicted from the friction model given the current vehicle speed and % slip

Equation 8-8 Calculation of vehicle acceleration from friction

$$V_t = V_{t-1} + (a_{t-1} \times \Delta t)$$

Where:

- V_t = the vehicle speed at time interval t
- V_{t-1} = The speed at the previous time interval (m/s)
- a_{t-1} = The acceleration at the previous time interval (m/s^2)
- Δt = The distance between the two time intervals (0.01 seconds in this example)

Equation 8-9 Calculation of speed

Distance travelled

The distance travelled at any time interval is calculated using the standard speed, distance and time relationship, this is shown in Equation 8-10.

$$d_t = V_t \times \Delta t$$

Where:

- d_t = the distance travelled at time interval t (m)
- Vt = the vehicle speed at time interval t (m/s)
- Δt = The distance between the two time intervals (0.01 seconds in this example)

Equation 8-10 Calculation of distance travelled

Summary

The iterative stages were repeated until the vehicle speed reached 20 km/h. The cumulative value of the distance travelled during the previous increments was then reported as the distance required for the vehicle to slow to 20 km/h.

Table 8-1 shows how the process was carried out and how each of the values were calculated using the equations shown in this chapter.

Table 8-1 Example of model

Parameter	Time	Wheel slip	Vehicle speed	Acceleration	Distance travelled	Friction
Unit	**(s)**	**(%)**	**(m/s)**	**(m/s^2)**	**(m)**	**None**
Symbol	**t**	**% Slip**	**V**	**A**	**d**	**Fn**
	0.00	2	V_1	Equation 8-8	Equation 8-10	Calculated from friction model
	0.01	IF ABS = No AND $t \leq t_p$ THEN Equation 8-3 ELSE Equation 8-4 OR IF ABS = Yes AND $t \leq t_p$ THEN Equation 8-6 ELSE Equation 8-7	Equation 8-9	Equation 8-3	Equation 8-6	Calculated from friction model
	n	As above	As above	As above	As above	As above

8.2 Assessment of vehicle demand and supply

The braking model was used to conduct a sensitivity analysis of the braking distance based on the friction supplied to motorists at different speeds and under different road conditions. The results have been compared with the braking distances quoted in the Highway Code.

8.2.1 Methodology

The braking model was used to estimate the distances required for a vehicle to slow to 20 km/h from initial speeds of 50, 75 and 100 km/h, with and without ABS, for various skid resistance and texture combinations. This will be referred to as the surface condition analysis.

The braking model was also used to estimate the distance required for a vehicle to slow to 20 km/h on the typical surface ranges defined in Chapter 6. This analysis allowed an investigation of the ability for different surface types in very good and very poor condition to slow a vehicle performing an emergency braking manoeuvre. This will be referred to as the surface type analysis.

For comparison, Figure 8-3 gives the relationship between stopping distance (without thinking time) in wet conditions, for various initial vehicle speeds, from the values given in the Highway Code (Department for Transport, 2004). Since the braking model is not able to estimate the braking distance below 20 km/h, the relationship in Figure 8-3 was

extrapolated, leading to an estimate of 4.71 m for the braking distance from 20 km/h. This was subtracted from the Highway Code braking distances for comparison with the results of the braking model.

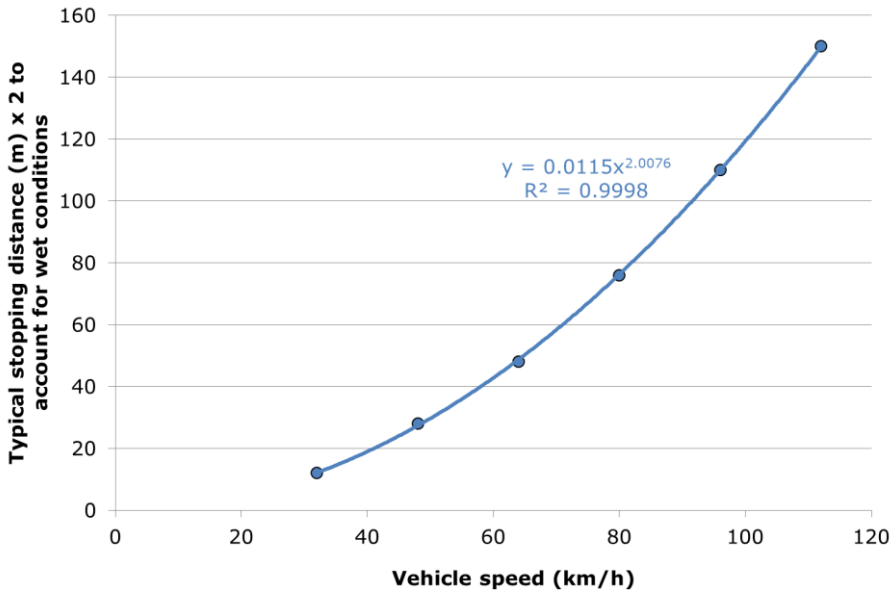

Figure 8-3 The relationship between initial vehicle speed and stopping distance (Department for Transport, 2004)

8.2.2 Results of the surface condition analysis

The results from the surface condition analysis are provided in Table 8-2 to Table 8-7. The values in the table cells represent the distance required to reduce the vehicle speed from the initial value to 20 km/h on pavements with the texture depth and low speed skid resistance characteristics represented by the row and column headers. The cells are shaded to indicate if the value is:

- <90% of the distance indicated by the Highway Code (Blue)
- ≥90 <100% of the distance indicated by the Highway Code (Orange)
- ≥ 100% of the distance indicated by the Highway Code (Red)

The texture depth requirement for the English SRN generally requires a level of above 0.8 mm SMTD (HD29 Data for pavement assessment, 2008). The skid resistance requirements are provided for different site categories in HD28 of the DMRB (HD28 Skidding resistance, 2015). Broadly, the site categories can be separated into two groups, high and low risk sites. The skid resistance requirements for low risk sites, such as mainline lengths of Motorways and All Purpose Trunk Roads are generally assigned a minimum Investigatory Level (IL) of 0.35 SC(50). The skid resistance requirements for high risk sites, such as approaches to junctions or roundabouts generally attract an IL of 0.50 SC(50). The texture depth and low speed skid resistance requirements for low and high risk sites are represented in the following tables by the dotted and solid thick lines respectively.

Initial speed 50 km/h

Table 8-2 Vehicle braking distance (m) to 20 km/h (V1 = 50, ABS used = Yes)

SC(50)	SMTD (mm)									
	0.2	0.4	0.6	0.8	1.0	1.2	1.4	1.6	1.8	2.0
0.20	39.07	25.56	20.52	17.98	16.32	15.18	14.52	13.89	13.31	12.89
0.25	34.89	23.15	18.94	16.71	15.26	14.42	13.69	13.09	12.59	12.19
0.30	31.43	21.27	17.55	15.75	14.49	13.59	12.90	12.38	11.96	11.67
0.35	28.47	19.57	16.45	14.72	13.60	12.86	12.25	11.89	11.50	11.19
0.40	25.92	18.13	15.40	13.87	12.87	12.28	11.77	11.37	10.99	10.76
0.45	23.70	16.95	14.40	13.18	12.29	11.69	11.30	11.00	10.70	10.42
0.50	21.58	15.73	13.62	12.48	11.80	11.27	10.89	10.58	10.29	10.08
0.55	19.78	14.79	12.99	11.98	11.28	10.81	10.47	10.18	9.91	9.70
0.60	18.32	14.00	12.31	11.40	10.81	10.39	10.08	9.80	9.58	9.39

Table 8-3 Vehicle braking distance (m) to 20 km/h (V1 = 50, ABS used = No)

SC(50)	SMTD (mm)									
	0.2	0.4	0.6	0.8	1.0	1.2	1.4	1.6	1.8	2.0
0.20	46.24	29.10	23.58	20.73	18.77	17.34	16.55	15.72	15.01	14.42
0.25	40.92	26.66	21.78	19.27	17.50	16.44	15.51	14.72	14.05	13.53
0.30	36.55	24.60	20.31	18.16	16.54	15.41	14.51	13.81	13.22	12.77
0.35	32.97	22.68	19.07	16.92	15.49	14.41	13.61	13.08	12.58	12.11
0.40	30.02	21.03	17.81	15.81	14.50	13.64	12.95	12.37	11.83	11.45
0.45	27.44	19.78	16.59	14.91	13.72	12.86	12.30	11.83	11.38	11.02
0.50	25.20	18.34	15.61	14.00	13.05	12.21	11.66	11.19	10.76	10.42
0.55	23.17	17.18	14.71	13.25	12.28	11.57	11.02	10.58	10.23	9.95
0.60	21.64	16.12	13.82	12.48	11.64	10.99	10.48	10.06	9.77	9.51

Initial speed75 km/h

Table 8-4 Vehicle braking distance (m) to 20 km/h (V1 = 75, ABS used = Yes)

	SMTD (mm)									
SC(50)	0.2	0.4	0.6	0.8	1.0	1.2	1.4	1.6	1.8	2.0
0.20	145.92	81.63	63.21	53.44	47.44	43.37	40.44	38.37	36.55	35.09
0.25	124.52	73.94	57.21	48.79	43.64	40.27	37.70	35.78	34.22	32.94
0.30	107.60	67.31	52.12	44.73	40.43	37.41	35.22	33.52	32.27	31.17
0.35	94.64	59.74	47.57	41.38	37.54	34.95	33.14	31.69	30.47	29.62
0.40	84.20	54.19	43.68	38.36	35.21	32.93	31.41	30.05	29.07	28.19
0.45	75.60	49.26	40.26	35.97	33.14	31.16	29.70	28.60	27.64	26.83
0.50	68.10	44.99	37.64	33.69	31.25	29.46	28.21	27.21	26.56	25.91
0.55	60.76	41.55	35.10	31.71	29.55	28.24	27.09	26.14	25.46	24.80
0.60	54.60	38.49	32.96	30.19	28.27	26.94	25.92	25.07	24.39	23.83

Table 8-5 Vehicle braking distance (m) to 20 km/h (V1 = 75, ABS used = No)

	SMTD (mm)									
SC(50)	0.2	0.4	0.6	0.8	1.0	1.2	1.4	1.6	1.8	2.0
0.20	221.70	102.36	78.04	66.34	59.33	54.42	50.72	48.13	45.80	43.89
0.25	173.87	91.41	71.16	61.15	54.88	50.75	47.51	44.98	42.85	41.11
0.30	143.93	82.49	65.23	56.48	51.17	47.32	44.39	42.07	40.35	38.81
0.35	123.01	74.76	60.05	52.58	47.70	44.20	41.73	39.64	37.94	36.65
0.40	107.46	68.30	55.69	48.89	44.65	41.55	39.32	37.44	35.95	34.65
0.45	95.41	62.80	51.64	45.83	41.93	39.14	36.99	35.34	33.92	32.71
0.50	85.57	57.87	48.27	42.87	39.39	36.82	34.90	33.35	32.28	31.31
0.55	77.22	53.71	45.04	40.23	36.99	34.95	33.20	31.72	30.64	29.65
0.60	70.29	49.93	42.20	38.02	35.16	33.05	31.47	30.17	29.03	28.18

Initial speed100 km/h

Table 8-6 Vehicle braking distance (m) to 20 km/h (V1 = 100, ABS used = Yes)

	SMTD (mm)									
SC(50)	0.2	0.4	0.6	0.8	1.0	1.2	1.4	1.6	1.8	2.0
0.20	411.94	232.18	141.16	129.31	107.82	90.15	83.13	77.95	73.80	70.45
0.25	341.10	207.95	138.79	110.79	97.73	82.50	76.49	71.98	68.44	65.66
0.30	291.16	172.77	123.79	100.12	86.51	75.84	70.78	67.04	64.02	61.50
0.35	254.01	143.32	106.53	91.39	76.18	70.30	66.42	63.11	60.42	58.24
0.40	225.33	127.26	96.64	81.36	71.00	65.87	62.14	59.23	56.91	54.97
0.45	188.47	109.80	88.59	72.47	66.03	61.61	58.34	55.82	53.74	52.05
0.50	165.08	99.30	76.29	67.27	61.76	57.95	55.07	52.79	51.05	49.55
0.55	147.00	90.72	70.89	62.85	58.02	54.63	52.09	50.17	48.56	47.23
0.60	125.34	78.60	65.99	59.41	54.76	51.88	49.59	47.80	46.37	45.15

Table 8-7 Vehicle braking distance (m) to 20 km/h (V1 = 100, ABS used = No)

	SMTD (mm)									
SC(50)	0.2	0.4	0.6	0.8	1.0	1.2	1.4	1.6	1.8	2.0
0.20	>452.31	261.07	184.29	151.31	132.75	119.57	110.57	103.91	98.41	93.95
0.25	>452.31	223.94	164.00	137.38	122.04	110.33	102.53	96.51	91.62	87.79
0.30	452.31	195.98	148.41	125.92	112.27	102.13	95.24	90.08	85.83	82.25
0.35	342.97	173.85	134.83	116.11	103.14	95.01	89.28	84.59	80.71	77.54
0.40	279.19	156.24	123.72	107.07	96.13	88.94	83.58	79.32	75.92	73.01
0.45	236.27	141.40	114.23	98.75	89.71	83.22	78.42	74.60	71.47	68.84
0.50	204.95	129.24	104.64	91.96	83.86	78.12	73.77	70.27	67.55	65.16
0.55	181.14	118.83	97.28	85.92	78.71	73.50	69.48	66.43	63.85	61.66
0.60	161.61	108.89	90.77	80.81	73.93	69.34	65.69	62.78	60.43	58.45

8.2.3 Results of the surface type analysis

The results from the surface type analysis are provided in Table 8-8. The values in the table cells represent the distance required to reduce the vehicle speed from the initial value (V1) to 20 km/h on the pavement types described by the row headers. The same shading as the previous tables has been used to indicate the surface performance against expected performance.

Table 8-8 Vehicle braking distances on different surface types

		Vehicle braking distance(m) to 20 km/h from following V1					
		With ABS			Without ABS		
Surface type		100	75	50	100	75	50
95th percentile (surface in good condition)	Concrete	69.52	34.85	12.53	91.82	43.32	13.90
	HRA	43.88	23.21	9.10	55.22	26.92	9.16
	TSCS	40.94	20.80	7.87	47.94	22.37	7.87
5th percentile (surface in poor condition)	Concrete	230.28	96.03	28.95	335.49	136.11	38.03
	HRA	116.55	58.59	21.10	172.65	84.44	28.93
	TSCS	83.06	42.32	16.60	134.27	62.04	21.69

8.2.4 Observations from results

From the results of this analysis the following general observations can be made:

- The braking distance is predicted to increase as either the low speed skid resistance or the texture depth decreases. Some combinations (indicated in red in the tables) result in a braking distance that exceeds the values given in the Highway Code.
- As modelled, the use of ABS results in a notable improvement in braking distance. (However, the model is relatively crude, assuming that the peak friction level is maintained throughout braking.)
- The margin between the area of the table corresponding to the friction requirements for Motorways and All Purpose Trunk Roads and the area of the table where the Highway Code braking distances are exceeded reduces with increasing vehicle speed.
- Arguably, pavements may be over specified, in terms of low speed skid resistance and texture, for sites where the speed limit is 50 km/h (30mph).
- The braking distance never exceeds Highways Code values for cases where the greatest texture depth (>= 1.1 mm SMTD) and low speed skid resistance (>= 0.5 SC(50)) requirements apply. This is not always the case for the lower requirements.
- It seems possible to mitigate the risk posed by low values of SC(50) with increasing texture depth, but the converse appears less achievable.

- Surfaces of all types kept in good condition provide lower braking distances than those given in the Highway Code.
- It may be expected for a TSCS in poor condition to provide acceptable braking performance, provided that the vehicle using the surface is equipped with ABS.

These results represent the worst case scenario (a vehicle with bald tyres and where locked-wheel friction is reached as soon as possible) and therefore may not be representative of the majority of the vehicle fleet.

9 Summary, discussion and conclusions

This chapter discusses the results of the work in the context of the research aims listed in Chapter 3.

9.1 Literature review

A literature review was carried out to further the knowledge of the influence of surface characteristics on vehicle handling under different manoeuvres. The study concluded that:

- Texture depth is a major contributor to friction at high levels of wheel slip, tyre properties and road surface microtexture contribute to friction at lower levels of slip.
- The most commonly reported road friction models use an exponential function to describe the change in friction with wheel slip percentage or vehicle speed.
- Driver aids generally operate in the region of the friction/slip curve around (at comparable slip ratios to) the peak friction.
- Vehicle dynamics systems contain proprietary algorithms for estimating the friction available. They make use of vehicle based information to make relatively crude assumptions about the maximum level of friction available.

9.2 Defining the speed, wheel slip and friction relationship

A procedure was developed for defining the friction profile of a road surface as a function of the test speed and wheel slip percentage. This procedure enabled the variation of friction to be observed readily over the range of achievable vehicle speeds and wheel slip ratios for individual surfaces. This is a substantial development as, traditionally, skid resistance is measured at a single vehicle speed and wheel slip percentage.

These three dimensional relationships were developed using historical measurements made using the PFT, available in a database maintained by TRL. In total 2,494 PFT measurements made on 169 surfaces between 1997 and 2013 were used in this study. Each surface was characterised over a speed range of 20 to 100 km/h at slip ratios between 2 and 100%.

The expression of pavement skid resistance as a function of vehicle speed and wheel slip is the first step in understanding the relationship between vehicle behaviour and pavement performance and, hence, assessing road user risk.

9.3 Assessment of typical material performance as a function of texture depth and low speed skid resistance

The friction profiles for different surface types were analysed to assess the typical range of performance for Concrete, HRA and TSCS materials. This was achieved by grouping the results collected from various materials and calculating the 5^{th} and 95^{th} percentiles of the friction values at each speed/slip combination.

This analysis identified a clear difference in performance between the materials. Concrete materials provided the lowest friction values of the three; the performance of the asphalt materials, TSCS and HRA, was generally higher than that of concrete. The 5^{th} percentile

performance of the asphalt materials was similar but the TSCS provided a greater 95th percentile, resulting in a large 90th percentile range. This variation may reflect the variability between TSCS materials, which are diverse and utilise different sizes of aggregate and binder materials.

A valuable sequel to this work would be to collect supplementary measurements of material performance on a variety of TSCS materials. This would enable the assessment of materials with different components or constructions.

It is likely that the overall performance of these materials is largely driven by their texture depth performance. Concrete surfaces tend to possess lower texture depth than asphalt materials, which could potentially lead to a poorer high speed friction performance. The implications for braking performance are discussed below in Section 9.5.

9.4 Development of a friction prediction model

A model was developed to predict the friction performance of materials with respect to wheel slip and vehicle speed, using input variables of low speed skid resistance and texture depth. This model was needed to estimate the implications of delivering different levels of low speed skid resistance and texture depth, which is discussed in Section 9.5.

The results of the modelling exercise were promising in relation to the current Highways England pavement assessment methodology since the parameters routinely measured by Highways England are capable of being used to infer friction performance with a reasonable level of accuracy. However there is scope for improving the model and the distribution of the residual values suggest that there are pavement properties other than texture depth and low speed skid resistance which influence friction generation.

Analysis of the residual values showed some discrepancies between actual and predicted values for very low levels of wheel slip and low speed skid resistance:

- At very low wheel slip, 2 to 5 %, the model has a tendency to under-estimate the amount of friction provided by the road surface.
- At low levels of low speed skid resistance, around 0.30 SC(50), the model tends to over-predict the amount of friction available by approximately 0.05 units.

This suggests that either the form of the equations used within the model is not accurately representing the influence of these parameters over this range, or some other influence is occurring that has not been included in the model. Further assessment of this phenomenon would be a valuable exercise for future work.

An analysis of the residual values from the friction model showed that the model was capable of predicting 95% of the friction values within 20 units. This performance is worse than that of the model reported in TRL367 (Roe *et al.*, 1998), which is capable of predicting 95% of friction values within 12 units. However, the TRL367 model predicts friction for only

one wheel slip and vehicle speed combination[B] whereas the model developed as part of this work is capable of predicting friction over a wide range of vehicle speed and wheel slip.

9.5 Significance of low speed skid resistance and texture for vehicle manoeuvres

A methodology was developed to assess the contribution of pavement texture depth and low speed skid resistance to the performance of vehicles conducting an emergency braking manoeuvre. This uses the deceleration that could be expected based on the friction model as a proxy for vehicle performance, to predict the distance required to slow a vehicle from a specified initial speed to 20 km/h. This exercise was carried out to model surfaces with varying texture depth and low speed skid resistance. The results were compared with the braking distances listed in the UK Highway Code.

The surface performance was analysed in the context of Highways England requirements for pavement texture depth and low speed skid resistance. The results showed that in all cases, the predicted braking performance supplied by pavements which met texture depth requirements of 0.8 mm SMTD and low speed skid resistance criteria of 0.50 SC(50) was within the distances listed in the Highway Code. The results also showed that at low vehicle speeds (50 km/h) the potential friction supply was markedly greater than that which may be demanded. This was, notably, not the case for braking manoeuvres from high speed with no ABS on pavements with lower requirements (0.8 mm SMTD and 0.35 SC(50)). It should be noted that these results represent a worst case scenario (i.e. a vehicle with bald tyres and where locked-wheel friction is reached as soon as possible).

An additional analysis was carried out to assess the performance of Concrete, HRA and TSCS materials in good (95th percentile) and poor (5th percentile) condition. The results of this analysis showed that all of the materials in good condition provided braking distances within those listed in the UK Highway Code. For HRA and Concrete in poor condition, the braking distance is generally predicted to be longer than given in the Highway Code. This is also the case for TSCS for the model without ABS although, notably, even in poor condition the TSCS seems to provide adequate braking with ABS.

While the exact threshold of the Highway Code distances should not be interpreted too literally given the number of assumptions made in the modelling, the observation suggests that in some areas of the network the pavement properties may be over specified whereas in other cases, pavements with low texture depth may not be providing satisfactory performance. Furthermore, the influence of speed is considerable. Speed is taken into account in specifying some site categories and Investigatory Levels within HD28, but this could be developed more thoroughly using this approach. Conversely, the risk on the network could be normalised by reducing traffic speed at high risk locations through the imposition of lower speed limits.

The analysis enabled the relative influence of texture depth and low speed skid resistance on the ability for a vehicle to conduct emergency braking to be assessed. This showed

[B] A vehicle speed of 100 km/h and 100% wheel slip (locked-wheel).

texture depth to be the dominant factor in reducing the distance required for a vehicle to slow to 20 km/h. In all of the cases observed, for materials simulated with low values of texture depth, an unrealistic amount of low speed skid resistance would be required to compensate for the loss of braking performance associated with the low texture depth. However for materials simulated with low values of low speed skid resistance, the loss of performance could be mitigated by the provision of, in most cases, an achievable level of texture depth.

This observation has potential connotations for pavement design and maintenance, but the assessment made was limited to a single manoeuvre, using a friction model based on measurements obtained from testing with a smooth tyre and a nominal 1mm water depth. It would be valuable, therefore, to carry out the same analysis for other manoeuvres such as, cornering, lane changes and combined braking and cornering. If similar observations are made then the results could be used to influence design and maintenance standards.

9.6 Conclusions

A procedure was developed, using historical measurements made with the PFT, for defining the friction profile of a road surface as a function of the test speed and wheel slip percentage. The resulting 3-dimensional friction profiles allowed the production of a model capable of predicting road pavement friction based on macrotexture and low speed skid resistance. The model also facilitates an understanding of how the road surface characteristics influence vehicle performance; in this case this has been studied through considering the effect of skid resistance and texture depth on vehicle braking manoeuvres from different initial speeds. This methodology could be extended to other manoeuvres following the collection of supporting vehicle dynamics information.

From the work carried out the following conclusions can be made:

- Concrete and asphalt materials exhibit markedly different friction performance. Further work should be undertaken to assess the effect of material design on the friction performance of TSCS materials, which varies considerably.
- The friction prediction model developed performs well overall in predicting friction over a wide range of slip ratio and vehicle speed, from inputs of low speed skid resistance and texture depth. However, it is less accurate at low slip (below 5%) and low, low speed friction (around 0.30 units SC(50)).
- Whilst low speed skid resistance and texture depth both contribute to the braking performance, the importance of texture depth seems particularly significant and texture depth is better able to compensate for lower levels of low speed skid resistance than vice versa.
- There appears to be an optimum contribution of low speed skid resistance and texture depth to braking distance, taking account of the vehicle speed and the performance of different surfacing materials.
- The use of driver aids designed to exploit peak friction has a substantial benefit on the braking performance of vehicles. A wide uptake (approaching 100%) of driver aids could allow for a reduction in the friction requirements on the SRN. However,

information on the current and projected distribution of vehicles with driver aids would be needed before making changes to specifications.

References

Aly AA, Zeidan ES, Hamed A and Salem F (2011). *An Antilock-Braking Systems (ABS) Control: A Technical Review* (2011 - 2 - 186-195). Scientific Research, Intelligent Control and Automation .

ASTM (2008). *E524-08 Standard Specification for Standard Smooth Tire for Pavement Skid-resistance Tests*. ASTM: West Conshohocken.

ASTM (2011). *E274/E274M-11 Standard Test Method for SkidResistance of Paved surfaces Using a full-Scale Tire*. ASTM: West Conshohocken.

ASTM (2015). *E1845-15 Standard practice for calculating pavement macrotexture measn profile depth*. ASTM: West Conshohocken.

ASTM (2015). *E965-15 Standard test method for measuring pavement macrotexture depth using a volumetric technique*. ASTM: West Conshohocken.

Brittain S and Viner HE (2017). *PPR818 Development of a high speed friction performance criteriion for asphalt materials* (Wokingham). TRL Limited.

BSI (2000). *BS 7941-2 Surface friction of pavements - Part 2: Test method for measurement of surface skid resistance using the GripTester braked wheel fixed slip device*. British Standards Institution: London.

BSI (2006). *BS 7941-1 Methods for measuring the skid resistance of pavement surfaces. Sideway-force coefficient routine investigation machine*. British Standards Institution: London.

Department for Transport (2004). *The highway code*. Department for Transport: London.

Flintsch GW, McGhee KK, de León Izeppi E and Najafi S (2012). *The little Book of Tire Pavement Friction Version 1.0*. Pavement Surface Properties Consortium.

Gothie M, Parry T and Roe P (2001). The relative influence of the parameters affecting road surface friction. 2nd International colloquium on vehicle tyre road interaction. University of Florence, Civil Engineering Department.

Hall JW, Smith KL, Tirus-Glover L, Wambold JC, Yager TJ and Rado Z (2009). *NCHRP Guide for Pavement Friction.*, National Cooperative Highway Research Program; Transport Research Board of the national academies, Contractor's Final Report for NCHRP Project 01-43.

Hart P (2003). *ABS Braking Requirements*. Hartwood Consulting Pty Ltd: Vistoria.

Henry JJ (1983). *Comparison of Friction Performance of a Passenger Tire and the ASTM Standard Test Tires, ASTM STP 793*. American Society for Testing and Materials (ASTM): Philadelphia, Pennsylvania.

Henry JJ (2000). *Evaluation of pavement friction characteristics*. Transportation Research Board.

Highways England, Transport Scotland, Welsh Government, The Department for Regional Development Northern Ireland (2006). *HD36 Surfacing materials for new and maintenance construction*. The Stationary Office: London.

Highways England, Transport Scotland, Welsh Government, The Department for Regional Development Northern Ireland (2008). *HD29 Data for pavement assessment*. The Stationery Office: London.

Highways England, Transport Scotland, Welsh Government, The Department for Regional Development Northern Ireland (2015). *HD28 Skidding resistance*. The Stationery Office: London.

Kane M, Conter M, Roe P and Schwalbe G (2009). *Report on different parameters influencing skid resistance, rolling resistance and noise emissions*. Deliverable D10 of the FP7 TYROSAFE project, available from http://www.transport-research.info/sites/default/files/project/documents/20120406_002134_64278_TYROSAFE_WP3_D10_ReportOnInfluencingParameters_v2.0_20090824.pdf.

Koskinen S and Peussa P (2004). *FRICTION - Final Report* (FP6-IST-2004-4-027006). Information Society Technologies Programme.

Kummer HW (1966). *Unified theory of rubber and tire friction*. Pennsylvania State University College of Engineering.

Manual of Contract documents for Highway Works. 2008.

Matsuzaki R, Kamai K and Seki R (2015). *Intelligent tires for identifying coefficient of friction of tire/road contact surfaces using three-axis accelerometer*. Smart Materials and Structures, Tokyo University of Science: 025010.

Moore DF (1975). *The friction of pneumatic tyres*. Elsevier Scientific Publishing Company: Amsterdam.

Pacejka HB (2006). *Tire and Vehicle Dynamics; Second Edition.*, SAE Society of Automotive Engineers.

Parry AR and Viner HE (2005). *TRL622 Accidents and the skidding resistance standard for strategic roads in England*. TRL: Wokingham.

Roe PG and Sinhal R (1998). *TRL322 The Polished Stone Value of aggregates and in-service skidding resistance*. TRL: Crowthorne, UK.

Roe PG, Parry AR and Viner HE (1998). *TRL367 High and low speed skidding resistance: the influence of texture depth*. TRL: Wokingham.

Roe PG and Dunford A (2012). *PPR564 The skid resistance behaviour of thin surface course systems*. TRL: Crowthorne, UK.

Sanders PD, Morosiuk K and Peeling J (2014). *PPR727 Road Surface properties and high speed friction*. TRL: Crowthorne.

Singh KB and Taheri S (2015). *Estimation of tire-road friction coefficient and its application in chassis control systems*. Systems Science & Control Engineering, 3:1, 39-61, DOI: 10.1080/21642583.2014.985804.

Vos E, Groenendijk J, Do MT and Roe P (2009). *Report on analysis and findingss of previous skid resistance harmonisation projects*. D05 Tyre and road surface optimisation for skid resistance and further effects.

Wallbank C, Viner H, Smith L and Smith R (2016). *The relationship between collisions and skid resistance on the Strategic Road Network*. TRL Limited: Wokingham.

Wang H, Al-Qadi IL and Staniculescu I (2010). *Effect of Friction on Rolling Tire - Pavement Interaction*. Nextrans.

Wong JY (1993). *Theory of Ground Vehicles.*, John Wiley & Sons, Inc.

Appendix A Summary of materials assessed and friction profiles generated

Profile number	Date of measurement	Measurements made	Location	Surfacing type
027	01/01/1997	15	A1	Thin Surface Course System
028	01/01/1997	16	A1	Thin Surface Course System
029	01/01/1997	16	A1	Exposed aggregate concrete
030	01/01/1997	16	A1	Exposed aggregate concrete
031	01/01/1997	16	A1	Exposed aggregate concrete
032	01/01/1997	15	A1	Stone mastic asphalt
033	01/01/1997	14	A329M	Hot rolled asphalt
034	01/01/1997	16	A329M	Hot rolled asphalt
035	01/01/1997	14	A329M	Hot rolled asphalt
036	01/01/1997	14	A329M	Hot rolled asphalt
037	01/01/1997	12	A329M	Exposed aggregate concrete
038	01/01/1997	12	A329M	Exposed aggregate concrete
039	01/01/1997	12	A329M	Exposed aggregate concrete
040	01/01/1997	12	A329M	Exposed aggregate concrete
041	01/01/1997	12	A329M	Hot rolled asphalt
042	01/01/1997	10	A329M	Thin Surface Course System
043	01/01/1997	14	M5	Hot rolled asphalt
044	01/01/1997	12	M5	Hot rolled asphalt
045	01/01/1997	14	M5	Hot rolled asphalt
046	01/01/1997	14	M5	Hot rolled asphalt
047	01/01/1997	14	M5	Hot rolled asphalt
048	01/01/1997	14	M5	Exposed aggregate concrete
051	01/01/1997	13	M5	Hot rolled asphalt
052	01/01/1997	13	M5	Hot rolled asphalt
053	01/01/1997	15	A140	Brushed concrete
054	01/01/1997	15	A140	Brushed concrete
055	01/01/1997	15	A140	Brushed concrete
056	01/01/1997	15	A140	Grooved concrete
057	01/01/1997	15	A140	Brushed concrete
058	01/01/1997	17	A140	Brushed concrete
059	01/01/1997	16	A140	Brushed concrete
060	01/01/1997	17	A140	Brushed concrete
061	01/01/1997	17	A140	Brushed concrete

Profile number	Date of measurement	Measurements made	Location	Surfacing type
062	01/01/1997	16	A140	Brushed concrete
069	01/01/1997	18	M40	Porous asphalt
070	01/01/1997	18	M40	Porous asphalt
071	01/01/1997	18	M40	Porous asphalt
072	01/01/1997	18	M40	Porous asphalt
073	01/01/1997	18	M40	Porous asphalt
074	01/01/1997	18	M40	Stone mastic asphalt
075	01/01/1997	18	M40	Stone mastic asphalt
076	01/01/1997	18	M40	Stone mastic asphalt
077	01/01/1997	16	M40	Stone mastic asphalt
078	01/01/1997	15	M40	Stone mastic asphalt
082	01/01/1997	14	A331	Porous asphalt
083	01/01/1997	14	A331	Hot rolled asphalt
084	01/01/1997	15	A322	Surface dressing
085	01/01/1997	15	A322	Surface dressing
086	01/01/1997	14	A322	Surface dressing
087	01/01/1997	15	A322	Surface dressing
088	01/01/1997	13	TRL	Exposed aggregate concrete
089	01/01/1997	12	TRL	Exposed aggregate concrete
091	01/01/1997	9	A249	Brushed concrete
092	01/01/1997	15	A249	Brushed concrete
093	01/01/1997	14	A249	Brushed concrete
094	01/01/1997	15	A249	Brushed concrete
095	01/01/1997	15	A249	Brushed concrete
096	01/01/1997	12	A249	Brushed concrete
097	01/01/1997	13	A27	Brushed concrete
098	01/01/1997	13	A27	Brushed concrete
099	01/01/1997	12	A27	Brushed concrete
100	01/01/1997	13	A27	Brushed concrete
101	01/01/1997	11	A27	Grooved concrete
102	01/01/1997	13	A27	Brushed concrete
103	01/01/1997	12	A27	Brushed concrete
104	01/01/1997	12	A27	Brushed concrete
105	01/01/1997	10	A27	Brushed concrete
106	01/01/1997	11	A325	Surface dressing
107	01/01/1997	12	A325	Surface dressing

Profile number	Date of measurement	Measurements made	Location	Surfacing type
108	01/01/1997	12	A325	Surface dressing
109	01/01/1997	12	A325	Surface dressing
110	01/01/1997	11	A325	Surface dressing
111	01/01/1997	15	A34	Brushed concrete
112	01/01/1997	15	A34	Brushed concrete
113	01/01/1997	15	A34	Brushed concrete
114	01/01/1997	14	A34	Brushed concrete
115	01/01/1997	15	A34	Hot rolled asphalt
116	01/01/1997	15	A90	Surface dressing
118	01/01/1997	15	A90	Surface dressing
119	01/01/1997	15	A90	Surface dressing
121	01/01/1997	15	A766	Hot rolled asphalt
122	01/01/1997	15	A766	Hot rolled asphalt
123	01/01/1997	15	A766	Surface dressing
124	01/01/1997	15	A766	Surface dressing
125	01/01/1997	15	A702	Hot rolled asphalt
126	01/01/1997	15	A702	Hot rolled asphalt
127	01/01/1997	12	A90	Grooved concrete
128	01/01/1997	12	A90	Grooved concrete
129	01/01/1997	14	A90	Brushed concrete
130	01/01/1997	115	A90	Brushed concrete
131	01/01/1997	14	A90	Brushed concrete
132	01/01/1997	15	A90	Brushed concrete
133	01/01/1997	14	A1_H	Stone mastic asphalt
134	01/01/1997	16	A1_H	Stone mastic asphalt
135	01/01/1997	16	A1_H	Stone mastic asphalt
136	01/01/1997	16	A1_H	Stone mastic asphalt
137	01/01/1997	16	A1_H	Stone mastic asphalt
138	01/01/1997	16	A1-M1	Brushed concrete
139	01/01/1997	15	A1-M1	Brushed concrete
140	01/01/1997	15	A1-M1	Brushed concrete
141	01/01/1997	15	A1-M1	Brushed concrete
143	06/12/2005	9	A5	Thin Surface Course System 10mm
144	06/12/2005	9	A5	Thin Surface Course System 14mm
145	06/12/2005	9	A5	Thin Surface Course System 14mm
151	23/06/2006	7	A5	Thin Surface Course System 10mm

Profile number	Date of measurement	Measurements made	Location	Surfacing type
152	23/06/2006	12	A5	Thin Surface Course System 14mm
153	23/06/2006	9	A5	Thin Surface Course System 14mm
154	23/06/2006	9	A5	Thin Surface Course System 6mm
155	23/06/2006	8	A5	Thin Surface Course System 10mm
156	23/06/2006	8	A5	Thin Surface Course System 14mm
170	22/06/2006	16	A5	Thin Surface Course System 10mm
171	22/06/2006	20	A5	Thin Surface Course System 14mm
172	22/06/2006	7	A5	Thin Surface Course System 10mm
173	22/06/2006	6	A5	Thin Surface Course System 14mm
174	04/10/2006	18	A5	Thin Surface Course System 10mm
175	04/10/2006	8	A5	Thin Surface Course System 14mm
176	04/10/2006	10	A5	Thin Surface Course System 10mm
177	04/10/2006	10	A5	Thin Surface Course System 14mm
179	02/06/2006	10	A14	Thin Surface Course System 10mm
180	02/06/2006	7	A14	Thin Surface Course System 14mm
181	03/06/2006	16	A14	Thin Surface Course System 6mm
182	03/06/2006	11	A14	Thin Surface Course System 10mm
183	03/06/2006	12	A14	Thin Surface Course System 14mm
186	20/10/2006	17	A14	Thin Surface Course System 14mm
188	12/11/2008	13	M8	Dense Thin Surface Course System 10mm un-gritted
189	12/11/2008	21	M8	Dense Thin Surface Course System 8mm un-gritted
190	12/11/2008	9	M8	Dense Thin Surface Course System 6mm un-gritted
193	12/11/2008	9	M8	Dense Thin Surface Course System 10mm gritted
195	16/11/2008	9	M8	Dense Thin Surface Course System 14mm un-gritted
196	16/11/2008	9	M8	Dense Thin Surface Course System 10mm un-gritted
197	16/11/2008	9	M8	Dense Thin Surface Course System 8mm un-gritted
200	16/11/2008	9	M8	Dense Thin Surface Course System 8mm gritted
220	30/08/2011	24	M27 EB	Pavement quality concrete
221	30/08/2011	9	M27	Pavement quality concrete (fine milling)
222	30/08/2011	19	M27	Pavement quality concrete (shot blasting)

Profile number	Date of measurement	Measurements made	Location	Surfacing type
223	30/08/2011	12	M27	Pavement quality concrete (bush hammering)
224	16/11/2011	11	M27 WB	Pavement quality concrete (fine milling)
227	16/11/2011	11	M27	Pavement quality concrete (shot blasting)
229	16/11/2011	13	M271 N	Pavement quality concrete (fine milling)
230	16/11/2011	24	M271 N	Pavement quality concrete (fine milling)
233	18/09/2012	15	M27 WB	Pavement quality concrete (fine milling)
234	18/09/2012	14	M27 EB	Pavement quality concrete (fine milling)
235	18/09/2012	14	M27	Pavement quality concrete (fine milling)
237	18/09/2012	14	M27	Pavement quality concrete (bush hammering)
238	18/09/2012	13	M271 N	Pavement quality concrete (fine milling)
239	18/09/2012	15	M271 N	Pavement quality concrete (fine milling)
240	18/09/2012	14	M271 S	Pavement quality concrete (fine milling)
241	18/09/2012	15	M271 S	Pavement quality concrete (fine milling)
242	19/06/2013	12	M27 WB	Pavement quality concrete (fine milling)
243	19/06/2013	12	M27 EB	Pavement quality concrete (fine milling)
244	19/06/2013	12	M27	Pavement quality concrete (fine milling)
245	19/06/2013	15	M27	Pavement quality concrete (shot blasting)
246	19/06/2013	13	M27	Pavement quality concrete (bush hammering)
247	19/06/2013	14	M271 N	Pavement quality concrete (fine milling)
248	19/06/2013	12	M271 N	Pavement quality concrete (fine milling)
249	19/06/2013	12	M271 S	Pavement quality concrete (fine milling)
251	01/10/2013	13	M27 WB	Pavement quality concrete (fine milling)
252	01/10/2013	10	M27 EB	Pavement quality concrete (fine milling)
255	01/10/2013	15	M27	Pavement quality concrete (bush hammering)
257	01/10/2013	15	M271 N	Pavement quality concrete (fine milling)
258	01/10/2013	15	M271 S	Pavement quality concrete (fine milling)
259	01/10/2013	15	M271 S	Pavement quality concrete (fine milling)
260	06/11/2012	28	M20/A20 EB	Pavement quality concrete (fine milling)
261	06/11/2012	34	M20/A20 EB	Pavement quality concrete (fine milling)
262	06/11/2012	30	M20/A20 WB	Pavement quality concrete (fine milling)
263	06/11/2012	28	M20/A20 WB	Pavement quality concrete (fine milling)
264	25/09/2013	22	A46	Pavement quality concrete (bush hammering)
265	25/09/2013	18	A46	Pavement quality concrete (longitudinal diamond grinding)
268	25/09/2013	24	A46	Pavement quality concrete (fine milling)

Appendix B Friction model coefficients

% Slip (x)	a	b	c	d
2	34.87	-11.77	10.17	37.70
3	52.24	-23.56	15.00	57.14
4	76.78	-39.48	18.80	67.29
5	100.74	-55.91	21.18	74.68
6	122.14	-70.75	22.79	79.22
7	135.23	-80.16	23.61	82.79
8	142.24	-85.27	23.96	84.82
9	147.32	-88.43	24.02	84.41
10	150.42	-90.29	23.95	83.72
11	152.22	-91.13	23.79	82.36
12	152.93	-91.35	23.64	81.31
13	152.97	-91.26	23.49	80.63
14	153.02	-91.11	23.29	79.62
15	153.23	-91.13	23.10	78.72
16	153.36	-90.94	22.87	77.34
17	153.44	-90.74	22.68	76.05
18	153.24	-90.47	22.41	75.11
19	152.90	-90.05	22.18	74.01
20	152.36	-89.58	21.91	73.12
21	151.96	-89.22	21.64	72.25
22	151.74	-88.96	21.37	71.31
23	151.63	-88.82	21.14	70.49
24	151.64	-88.70	20.90	69.49
25	151.44	-88.46	20.69	68.64
26	151.24	-88.24	20.49	67.83
27	151.05	-88.02	20.28	66.99
28	150.85	-87.81	20.10	66.22
29	150.66	-87.60	19.92	65.42
30	150.49	-87.40	19.78	64.58
31	150.30	-87.22	19.61	63.84
32	149.99	-87.02	19.42	63.32
33	149.83	-86.86	19.23	62.58
34	149.65	-86.67	19.08	61.85
35	149.37	-86.44	18.91	61.25
36	149.08	-86.17	18.78	60.56
37	148.72	-85.87	18.64	59.95
38	147.99	-85.45	18.49	59.75
39	147.64	-85.14	18.29	59.03
40	147.07	-84.70	18.11	58.41
41	146.20	-84.23	17.94	58.32
42	145.73	-83.88	17.73	57.72
43	145.04	-83.44	17.56	57.34
44	144.16	-82.92	17.39	57.14
45	143.51	-82.54	17.23	56.87
46	142.75	-82.07	17.10	56.58
47	142.22	-81.67	16.94	56.03
48	141.62	-81.31	16.79	55.71
49	141.08	-80.96	16.65	55.34
50	140.65	-80.66	16.52	54.89
51	140.21	-80.34	16.41	54.43
52	139.80	-80.03	16.27	53.94
53	139.29	-79.66	16.14	53.47
54	138.74	-79.24	16.04	52.96
55	138.21	-78.81	15.95	52.40
56	137.83	-78.44	15.82	51.63
57	137.24	-77.97	15.70	51.06
58	136.57	-77.46	15.60	50.52
59	135.91	-76.98	15.49	50.02
60	135.23	-76.47	15.38	49.49
61	134.61	-75.99	15.30	48.89
62	134.01	-75.59	15.21	48.60
63	133.05	-74.97	15.09	48.27
64	132.24	-74.50	14.98	48.05
65	131.73	-74.21	14.90	47.76
66	131.24	-73.90	14.84	47.39
67	130.65	-73.53	14.73	47.05
68	130.27	-73.29	14.66	46.64
69	130.09	-73.16	14.60	46.18
70	130.04	-73.07	14.54	45.61

% Slip (x)	a	b	c	d
71	130.09	-73.01	14.51	44.92
72	129.94	-72.83	14.44	44.22
73	129.84	-72.74	14.35	43.70
74	129.72	-72.72	14.26	43.35
75	129.49	-72.66	14.18	43.09
76	128.98	-72.43	14.10	42.92
77	128.51	-72.26	14.02	42.77
78	127.98	-72.13	13.95	42.87
79	127.37	-71.97	13.88	43.01
80	126.86	-71.96	13.80	43.27
81	126.73	-72.09	13.77	43.33
82	126.57	-72.15	13.70	43.29
83	126.35	-72.09	13.61	43.10
84	126.23	-71.91	13.50	42.47
85	125.97	-71.56	13.34	41.59
86	125.79	-71.32	13.21	40.95
87	125.81	-71.23	13.14	40.24
88	126.42	-71.76	13.12	39.82
89	127.47	-72.78	13.07	39.62
90	128.42	-73.83	13.03	39.65
91	129.86	-75.10	12.97	39.31
92	130.38	-75.66	12.92	39.22
93	130.15	-75.77	12.83	39.51
94	130.26	-75.97	12.82	39.38
95	130.28	-76.24	12.79	39.55
96	129.99	-76.33	12.81	39.86
97	129.67	-76.34	12.85	40.08
98	129.72	-76.63	12.90	40.31
99	129.79	-76.95	12.95	40.56
100	130.89	-77.91	12.95	40.41

Better understanding of the surface tyre interface

Other titles from this subject area

PPR806	The relationship between collisions and skid resistance on the Strategic Road Network. C Wallbank, H Viner, L Smith, R Smith. 2016
TRL 662	Accidents and the skidding resistance standard for strategic roads in England. A R Parry and H E Viner. 2005

TRL
Crowthorne House, Nine Mile Ride,
Wokingham, Berkshire, RG40 3GA,
United Kingdom
T: +44 (0) 1344 773131
F: +44 (0) 1344 770356
E: enquiries@trl.co.uk
W: www.trl.co.uk

ISSN

ISBN

PPR815